GEOLOGICA CARPATHICA, FEBRUARY 2022, 73, 1, 43–62 https://doi.org/10.31577/GeolCarp.73.1.3

The structural pattern and tectonic evolution of the Muráň fault revealed by geological data, fault-slip analysis, and paleostress reconstruction (Western Carpathians)

SILVIA GERÁTOVÁ[1,✉], RASTISLAV VOJTKO[1], ALEXANDER LAČNÝ[1,2] and KATARÍNA KRIVÁŇOVÁ[1]

[1]Department of Geology and Paleontology, Faculty of Natural Sciences, Comenius University in Bratislava, Ilkovičova 6, 842 15 Bratislava, Slovakia; ✉michalikova.silvia@gmail.com, rastislav.vojtko@uniba.sk, alexander.lacny@uniba.sk
[2]State Nature Conservancy of the Slovak Republic, Little Carpathians Protected Landscape Area, Štúrova 115, 900 01 Modra, Slovakia; alexander.lacny@sopsr.sk

(Manuscript received May 17, 2021; accepted in revised form January 4, 2022; Associate Editor: Ján Madarás)

Abstract: The Muráň fault is perhaps the most distinctive, steeply-dipping, brittle structure in the Western Carpathians. An analysis of brittle deformation was used to gain the succession of tectonic evolution of the Muráň fault by paleostress tensors. Movement on this fault depended on spatial orientation of the principal paleostress axes representing the paleostress fields. The kinematic analysis of fault-slip data confirmed the predominant strike-slip nature of the fault during the entire history, which had sometimes been disrupted by quiescence periods or normal faulting. The Muráň fault may be as old as 85 Ma and originated as a ductile shear zone in deeper crust. It is possible to consider the Muráň fault as sinistral transpressional strike-slip fault during the latest Cretaceous to earliest Paleocene. During this time period, with given orientation of the paleostress field, the fault originated as a semi-brittle to brittle shear zone. A significant re-organization of the paleostress field was carried out approximately on the boundary of the Paleocene and Eocene periods. During this deformation, movement on the Muráň fault changed to dextral, and the secondary positive and negative flower structures in Mesozoic rocks were most likely formed in this time as well. These structures originated after the Danian, since sediments of the Gosau Group are incorporated into these structures. In the late Eocene, activity of the Muráň fault gradually began to decrease, and the fault structure is more or less covered by the upper Eocene transgressive deposits of the Central Carpathian Paleogene Basin. The Neogene evolution is characterised by a continuous change of the orientation of the principal maximum axis σ_1 (S_{Hmax}, respectively) from the NW–SE through N–S to NE–SW position. The Muráň fault started to become sinistral transpressional to transtensional up to a normal fault, however, the movement along the fault was only several tens of metres. The Quaternary period is characterised by an extensional tectonic regime with the orientation of principal least axis σ_3 in the WNW–ESE direction. Late Pleistocene to Holocene normal faulting is indicated by borehole analysis in the alluvial planes of the Rimava and Muráň rivers.

Keywords: Western Carpathians, Muráň fault, fault-slip analysis, paleostress reconstruction, tectonic evolution.

Introduction

The study area is located in the southern part of the historical region of Spiš and the northern part of Gemer, approximately between Spišská Nová Ves and Tisovec towns (Fig. 1). This study is focused on the most expressed fault zone in the Central Western Carpathians. The Muráň fault was most likely described for the first time by Uhlig (1903) as "Murany-Dislokation" in Hungarian, or "Muranylinie" in German after the name of the Muráň Castle (Murány vár in Hungarian) or the village of Muráň (Murányalja falu in Hungarian) during the Habsburg Empire until 1918. The fault is a very long and straight NE–SW striking structure, several tens of metres wide, with a brittle to semi-brittle zone. The Muráň fault is probably the most distinctive steeply dipping structure in the Western Carpathians, conspicuous in remote sensing and the digital elevation model, as well as in geological maps (Fig. 1). The fault zone, together with accompanying dislocations, is evident as a pronounced feature in geophysical data as well (cf. Pospíšil et al. 1986, 1989; Putiška et al. 2012).

Fault-slip analysis and paleostress reconstruction of the Muráň fault by modern techniques was performed by Marko (1993), who recognised three tectonic regimes and interpreted the kinematics of the Muráň fault as having varied between sinistral, dextral strike-slip, and normal slip. These studies have been further supplemented and updated (Marko & Vojtko 2006; Pelech & Kronome 2019). The present article is based not only on the results of Vojtko (2003), but also on new structural work in the north-eastern part of the Muráň fault in the Vernár and Stratená nappes.

The Muráň fault has affected the Paleo-Alpine nappe stack, which was formed during the Early Cretaceous age (e.g., Maheľ 1986; Plašienka 1999, 2018), including the structures related to the unroofing of the Veporic metamorphic dome that occurred during the early Late Cretaceous (≈100–80 Ma) and was followed by a period of denudation (cf. Králiková et al. 2016; Vojtko et al. 2016). For this reason, the lower limit of

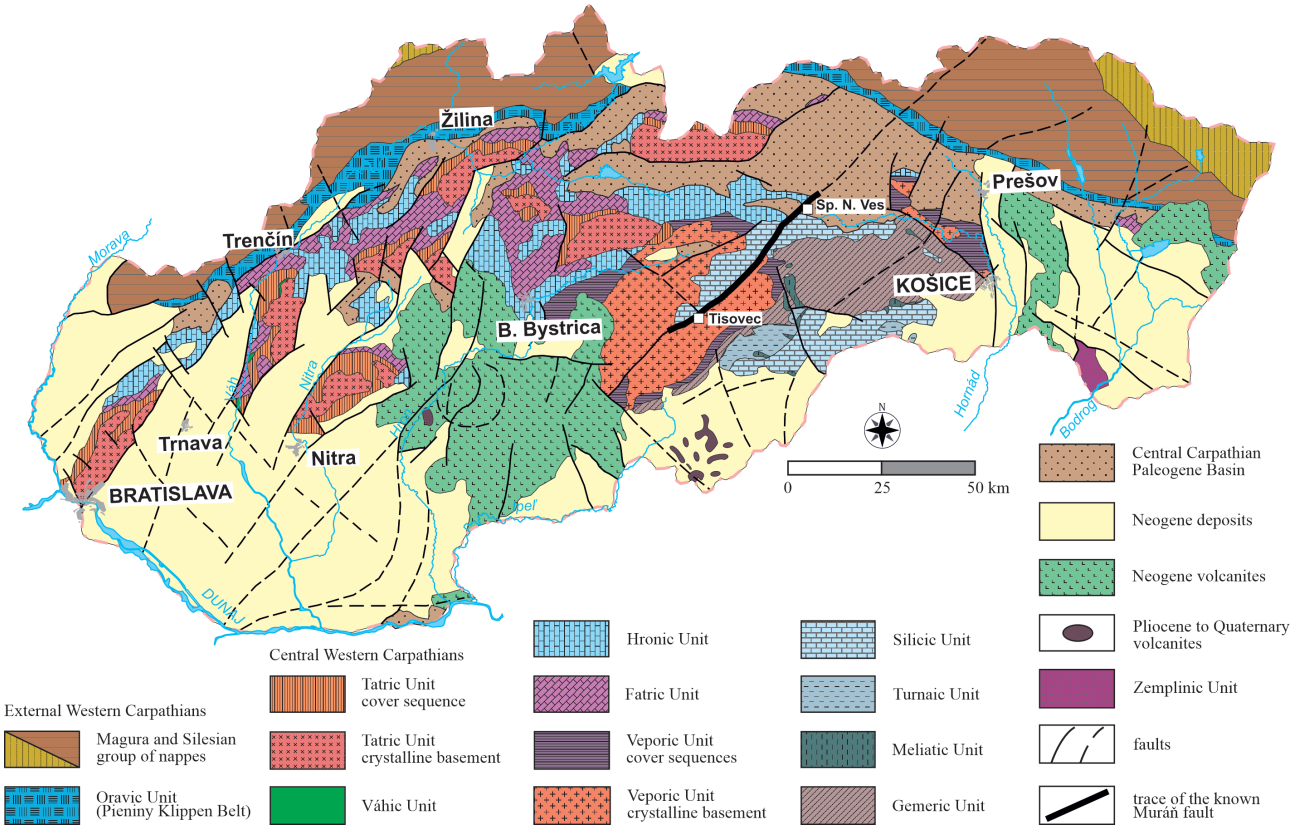

Fig. 1. Tectonic division of the Slovak part of the Western Carpathians with marking of the observed trace of the Muráň fault (according to Biely et al. 1996).

the fault zone formation is placed in the latest Cretaceous. Thus, the kinematic evolution of the Muráň fault mirrors the deformational processes of the latest Cretaceous to Cenozoic tectonic evolution, which occurred in the Central Western Carpathians. Several fault-related structures, including mesoscale ones, have been observed and analysed within the Muráň fault zone. This article summarises the knowledge concerning the orientation of paleostress axes determined from fault-slip data, tension gashes, and relationships of map-scale structures observed in the field or depicted on geological maps. We are not only interested in the orientation of the principal axes of the paleostress field, but especially in the kinematics and evolution of the Muráň fault and the main time span of its faulting activity. The principal aim of this study is to describe the tectonic evolution of this long-lived complex fault and its temporally-varying kinematics related to orientation of paleostress axes.

Methods

In the present study, the faults were the most important deformation structures that were analysed in detail. The relative movement orientation of the faults can be unambiguously determined using slickenside lineations on the slip surfaces. In many cases, this movement caused the evolution of asymmetric structures associated with the lineation, which clarifies not only the direction, but also the sense of the relative movement along the fault surface. This relative movement is expressed by kinematic indicators (Riedel 1929; Ramsay & Graham 1970; Hancock 1985; Hancock & Barka 1987; McClay 1987; Petit 1987; Park 1993).

The faults are commonly combined into systems with a given symmetry. The group of faults is defined on the basis of common geometry in relation to the strike and dip of the fault surfaces, as well as the trend and plunge of the lineation. Over the last 45 years, methodologies and routines for determining the relationships between stress and slip on fault surfaces have been progressively improved in order to determine the paleostress axes orientation. The relationship between stress axes and slip on fracture surfaces was firstly described in Wallace (1951) and Bott (1959).

The first attempt to formulate and solve the inverse problem was published in Carey & Brunier (1974), where the problem of shear stress orientation on various predisposed fault surfaces was solved, and the average reduced stress tensor was determined. Further work was not long in coming and since then, the development of methods has accelerated considerably (Angelier 1975, 1979, 1984, 1989, 1990, 1994; Armijo & Cisternas 1978; Etchecopar et al. 1981; Angelier et al. 1982;

Gephart & Forsyth 1984; Michael 1984; Célérier 1988; Célérier et al. 2012; Vavryčuk 2014).

The obtained data by field measurements were used in the Improved Right Dihedron and Rotational Optimization method implemented in the WinTensor software package developed by Damien Delvaux (Delvaux 1993; Delvaux & Sperner 2003). The Improved Right Dihedron method is based on the previously well-known Right Dihedron method, which was originally developed by Angelier & Mechler (1977) as a graphical method for the determination of the range of possible orientations of paleostress axes in fault-slip analysis. It provides a determination of the four parameters of the reduced stress tensor and also allows for a preliminary separation of the fault population into a homogeneous subset.

The Rotational Optimization is an inversion method, which is based on the assumption by Bott (1959) that slip on a plane occurs in the direction of the maximum resolved shear stress. The main problem consists of determining the orientation of the direction and sense of slip on the fracture surface for a given stress tensor. The entire inverse problem routine consists of determining the stress tensor, which relates to the direction and orientation of slip on the fault surface. In both cases, the basic condition is that each fault-slip indicated by the slickenside lineation has a direction and orientation of shear stress corresponding to a simple stress tensor, which is characterised by three main stress axes (σ_1, σ_2, and σ_3). The calculation of the reduced stress tensor makes it possible to determine the relationships between the magnitudes of these main stress axes (σ_1 maximum compressional stress axis; σ_2 intermediate stress axis, and σ_3 minimum compressional stress axis). This relationship is clearly expressed by the ratio of the main stress differences Φ, which can have values between 0 and 1, where $\Phi=(\sigma_2-\sigma_3)/(\sigma_1-\sigma_3)$ (Angelier 1975). The extreme cases are thus characterised by the extreme values $\Phi=0$ ($\sigma_2=\sigma_3$) and $\Phi=1$ ($\sigma_2=\sigma_1$).

Homogeneous populations of slickenside lineations for computation of single stress stages have to be separated and combined. And so, it is necessary to say that with regards to brittle deformation, the entire area of the Muráň fault zone is considered a homogeneous structural domain. As a discrimination criterion for separation of fault slips to homogeneous groups, an angle between theoretical and measured orientation of slickenside lineations on fault surfaces was used.

The stress regime is expressed numerically using an index Φ', ranking from 0.0 to 3.0 and defined as follows (see Delvaux et al. 1997): where the stress regime (Φ' between 0–1 for extensional regime, 1–2 for strike-slip regime, and 2–3 for compressional regime) are fully described by the average stress regime index Φ'.

Geological setting

The study area is composed of various Paleo-Alpine nappe units and post-nappe deposits with volcanic rocks (Fig. 2). Structurally, the lowermost nappe is related to the Veporic Unit, which is characterised as a thick-skinned thrust sheet formed by pre-Alpine crystalline basement rocks and their sedimentary cover sequences (Andrusov et al. 1973; Plašienka et al. 1997; Plašienka 1999, 2018; Janák et al. 2001; Lexa et al. 2003; Vojtko et al. 2016). The crystalline basement mostly contains lower Paleozoic metamorphosed volcano-sedimentary rocks that were intruded and overthrust by the voluminous Veporic granitoid pluton of Variscan age, mainly Late Devonian to early Carboniferous. The Alpine tectonogenesis with metamorphism significantly overprinted the original Variscan structures, especially in the southern part of the Veporic Unit (e.g., Vrána 1980; Kováčik et al. 1996; Janák et al. 2001; Jeřábek et al. 2008, 2012). Currently, the Veporic Unit can be subdivided into two tectonic subunits that differ by metamorphic grade and Mesozoic sedimentary cover (Figs. 2, 3): the lower, Northern, Veporic Subunit with its Veľký Bok cover sequence (Kettner 1931) and the upper, Southern, Veporic Subunit with its Foederata cover sequence (cf. Schönnenberg 1946; Plašienka 1993; Vojtko et al. 2015). Both units are divided by the Pohorelá fault (e.g., Zoubek 1957; Hók & Hraško 1990; Madarás et al. 1994; Hók & Vojtko 2011). While the Veľký Bok sequence is well-preserved and contains sedimentary strata from the Permian to mid-Cretaceous (Plašienka 2003), the Foederata is only rudimentarily preserved and ranges stratigraphically from the late Carboniferous to Late Triassic. Formations younger than the Triassic had never been proved until now (cf. Plašienka 1993; Vojtko et al. 2015).

The Veporic Unit is overridden by a thick-skinned imbricate thrust sheet with a complicated internal structure called the Gemeric Unit, which occurred during the Early Cretaceous shortening (Andrusov et al. 1973; Lexa et al. 2003). The basement is formed by metamorphosed lower Paleozoic rocks with upper Paleozoic to lower Mesozoic cover sequences and intruded by Permian granite intrusions (Poller et al. 2002; Radvanec et al. 2009; Broska & Kubiš 2018). It is conventionally divided into Southern and Northern Gemeric subunits (e.g., Vozárová & Vozár 1988). The differences between them are considerable, which is mainly documented by their lithological composition, but also by the different degrees of metamorphosis during the Variscan and Alpine tectono-metamorphic processes. The Gemeric Unit is represented by the Klátov Group, which consists of a gneiss-amphibolite complex, metamorphosed under the amphibolite facies during their Variscan orogeny (Faryad 1990; Radvanec et al. 2017). The Klátov Group is mostly covered by metabasites and phyllites metamorphosed under greenschist facies condition of the Rakovec Unit (cf. Faryad & Bernhardt 1996; Vozárová 1993). The lower Paleozoic basement of the Northern Gemeric Unit is covered by the Dobšiná Group (upper Carboniferous). This formation contains basal conglomerate, shallow sediments, basic volcanics and regression paralic formation of terrigenous deposits. These various complexes of the Northern Gemeric basement are transgressively-covered by the Krompachy Group (Permian). The group contains unsorted coarse-grained siliciclastic terrigeneous deposits with subalkaline rhyolite volcanic

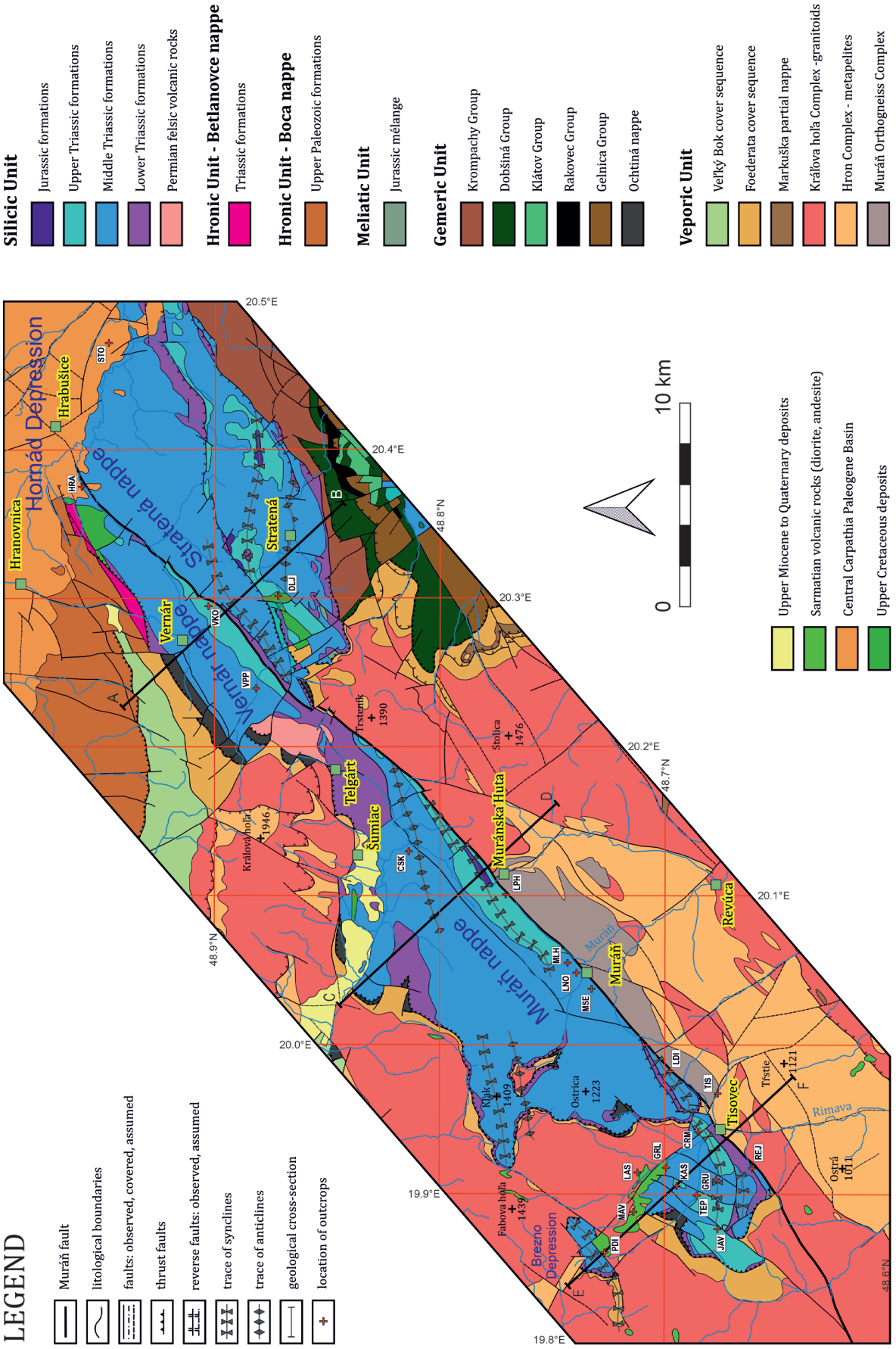

Fig. 2. Simplified tectonic map of the trace area of the Muráň fault between Hrabušice and Tisovec (according to Bezák et al. 2008; Mello et al. 2008). For the precise location of sites, see Table 1.

to volcaniclastic rocks, which pass to lagoon-sabcha sediments in the late Permian to Early Triassic (Vozárová & Vozár 1988; Vozárová & Rojkovič 2000). Both, the Veporic and Gemeric thick-skinned units overcame greenschists to amphibolite facies Alpine metamorphosis and are covered by an unmetamorphosed, thin-skinned, Vernár–Muráň–Stratená nappe system related to the Silicic Unit, as well as the Boca–Betlanovce nappe system related to the Hronic Unit (Figs. 2, 3).

The Silicic Unit includes the structurally highest, unmetamorphosed nappes of the region (Kozur & Mock 1973; Mello 1979). Based on their lithostratigraphy, the nappe system of the Silicic Unit can be correlated with the upper Tirolic and/or Juvavic nappes of the Eastern Alps. The palinspastic position of this unit is uncertain (e.g., Kozur & Mock 1973; Reichwalder 1982; Hók et al. 1995; Rakús 1996; Gawlick et al. 1999; Gawlick & Missoni 2015; Plašienka 2018). These nappes form internally-indistinctive, deformed thrust nappes, detached at the base of a thick upper Permian–Lower Triassic of mostly mixed, siliciclastic-carbonate rocks and evaporite-bearing horizon. However, tectonic duplexes of the Meliatic oceanic rocks were found at the base of the Stratená nappe and had been incorporated in places into evaporite mélanges (e.g., Havrila & Ožvoldová 1996; Mello et al. 2000b). In the study area, the Muráň–Vernár–Stratená nappe system (Figs. 2, 3) was dissected by later, transpressional movements along the deep-seated Muráň strike-slip fault system (e.g., Marko 1993; Pelech & Kronome 2019).

The soles of the Silicic-related nappes were formed by the upper Permian, evaporite-bearing Perkupa Formation and rauhwackised carbonate tectonic breccias overlain by Lower Triassic sandstones and shales passing upwards to marlstones and limestones (Plašienka & Soták 1996). Rhyolite volcanic rocks occur in the Muráň and Vernár nappe system, and their age was proved as Permian (Demko & Hraško 2013; Ondrejka et al. 2018). The Middle to Upper Triassic rocks represent a substantial part of the filling of the Silicic Unit. The Anisian carbonate platform was partly destroyed by a marked, Pelsonian rifting event, which led to the formation of intra-shelf basins filled with hemipelagic nodular limestones and resedimented carbonates (Kovács et al. 2011). These rocks were replaced by the Wetterstein carbonate platform in the late Ladinian to Cordevolian, which were disrupted by Julian fluvial events and the occurrence of siliciclastic turbidite-like deposits or marly limestone. The Late Triassic is characterised by huge carbonate platform complexes with extensive prograding, thick reef bodies surrounded by peri-reef bioclastic aprons, barrier reefs which grade into back-reef lagoonal flats. These shallow water deposits are occasionally overlain by Upper Triassic basinal and slope pelagic limestones and marlstones. The Jurassic members are, however, poorly preserved; their overall thickness reaches just several tens of metres (Vojtko 2000; Rakús & Sýkora 2001; Kronome & Boorová 2014). The youngest dated sediments of the Silicic nappe system are Callovian–Oxfordian in age.

The Upper Cretaceous to lower Paleogene sediments (Fig. 2) rest in an overstepping position over the Triassic–Jurassic carbonates of the Vernár, Stratená, and Muráň nappes (e.g., Klinec 1976; Mello et al. 2000a,b). In essence, they are considered to be an equivalent of the Gossau Group of the Eastern Alps. These sedimentary strata are composed of marine deposits of Late Cretaceous and mainly various siliciclastic, grain-sized deposits, predominantly polymictic conglomerates containing pebbles from superficial nappes and Upper Jurassic – Meliata related ophiolites (e.g., Mišík & Sýkora 1980; Hovorka et al. 1990).

A sedimentary succession of the late Eocene to late Oligocene age is connected to the Central Carpathian Paleogene Basin (cf. Gross et al. 1984). In the study area, these deposits are widespread in the Hornád Depression in the north and the Brezno Depression in the west (Fig. 2). Moreover, the Paleogene sediments are only sporadically widespread in the Horehronie Valley and rudimentary as erosive residue on top of the ridge northwest of Tisovec (Vojtko 2000; Plašienka & Soták 2001). The Central Carpathian Paleogene Basin is interpreted as a forearc basin located behind the Outer Western Carpathians accretionary wedge (Royden & Báldi 1988; Kázmer et al. 2003; Kováč et al. 2016; Plašienka 2018). The Paleogene sedimentary sequences lie discordantly on the Paleo-Alpine nappe structure. The basin is filled with several hundreds of meters of deep-marine siliciclastic sediments (Soták et al. 1996, 2001). Erosive remnants close to the town of Tisovec are considered equivalent to the Central Carpathian Paleogene Basin. However, their relation to the Buda Basin is not excluded (cf. Soták et al. 2005).

Unlike the Central Slovak and Eastern Slovak volcanic–plutonic complexes, where characteristic volcanic morphological features have been preserved, the uplift and erosion of the central part of the Veporské rudohorie Mts. has exposed the subvolcanic levels of the extinct volcano Sarmatian in age (Konečný et al. 2015a,b). Subvolcanic intrusive bodies, which predominantly vary in types of andesite and diorite, are scattered over an area of about 400 km^2, while the central zone of volcanic activity is located 5 km NW of the town of Tisovec and called the Tisovec Intrusive Complex (Figs. 2, 3; Bacsó 1964).

Fault-slip analysis and paleostress reconstruction

The formation of the Muráň fault is characterised by polyphase faulting. The reconstructions of the stress field evolution were solved by fault-slip analysis in various rocks with different age. In total, almost eight hundred fault-slips data were measured in twenty-two different sites (Table 1). Based on the fault-slip analysis and paleostress reconstruction, it was possible to determine eight independent deformational phases, all of which played an important role in the Late Cretaceous to Cenozoic evolution of the Muráň fault. The results of the structural analysis are listed in Table 2 and graphically drawn in Figs. 4–6. Paleostress reconstruction was performed in age-different rocks for the purpose of relative chronology of faulting during the Cenozoic era. The Sarmatian andesite and diorite of the Tisovec Intrusive Complex, which were out-

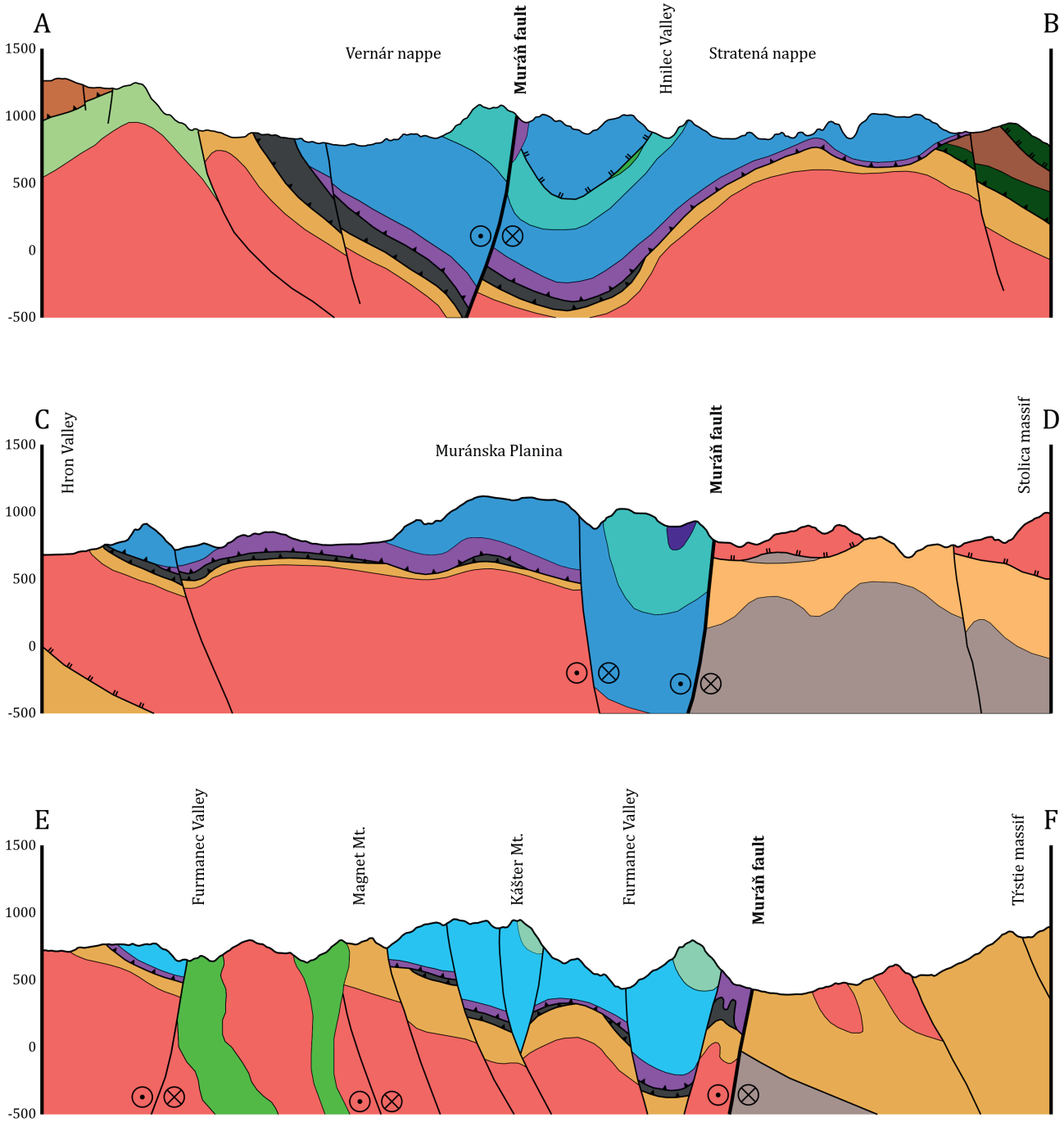

Fig. 3. Geological cross-sections through the trace area of the Muráň fault. Note: For explanation and location of geological cross-sections, see Fig. 2.

cropped in the northwest of the town of Tisovec, are the youngest rocks where structural measurements were performed (Figs. 2, 3). The age of the intrusive rocks was proved by $^{40}K/^{40}Ar$ ~12 Ma (Konečný et al. 2015a,b) and FT dating – 13.2±1.1 Ma (Vojtko et al. 2016). Structural measurements were also performed in older, upper Eocene to Oligocene formations of the Central Carpathian Paleogene Basin (cf. Gross et al. 1984; Soták et al. 1996, 2001). Very important data were obtained from the Upper Cretaceous sedimentary deposits and the crystalline basement of the Veporic Unit. These data were used as a discriminatory criterion for the chronology of faulting between the Late Cretaceous and middle Eocene. Finally, a large amount of structural data was obtained from the Triassic carbonates and siliciclastic sediments of the Muráň and Vernár nappes, especially from either abandoned or active quarries.

Table 1: General information and location of sites with measured fault-slip data. Note: VKO (Vernár – Kopanec) and VPP (Vernár – Pusté Pole) are composite sites, thus coordinates in the table represent only the most important outcrops.

Code	Longitude [easting]	Latitude [northing]	Name	Lithology	Age	Possible age of faulting
LAS	19.91444	48.71639	Lašťoky	Sarmatian volcanic rocks	12–13	<12 Ma
PDI	19.86083	48.73083	Pod Dielom quarry	Sarmatian volcanic rocks	12–13	<12 Ma
MAV	19.88806	48.71806	Magnetový vrch	Oligocene sediments	23–34	<23 Ma
STO	20.47194	48.95056	Ďurkovec quarry	upper Eocene sediments	33–35	<33 Ma
HRA	20.36888	48.96060	Hrabušice – Podlesok	upper Eocene sediments	34–35	<33 Ma
DLJ	20.30139	48.87583	Dobšinská Ľadová Jaskyňa	Upper Cretaceous sediments	65–86	<65 Ma
TIS	19.96750	48.68083	Tisovec – Dúhovo	Vepor crystalline basement	340–360	<80 Ma
JAV	19.87667	48.68083	Javorina	Dachstein Limestone	200–227	<200 Ma
CRM	19.94167	48.68944	Čeremošná	Dachstein Limestone	200–227	<200 Ma
TEP	19.89917	48.69000	Teplica	Dachstein Limestone	200–227	<200 Ma
LPH	20.10083	48.77500	Lom Predná Hora	Dachstein Limestone	200–227	<200 Ma
VKO	20.29461	48.90673	Vernár – Kopanec	Haupt Dolomite	200–227	<200 Ma
MLH	20.05500	48.74750	Muráň – Lom pod hradom	Wetterstein Dolomite	227–237	<227 Ma
LNO	20.04833	48.74361	Muráň – Lom nad obcou	Wetterstein Dolomite	227–237	<227 Ma
GRU	19.91000	48.68139	Grúniky	Wetterstein Dolomite	227–237	<227 Ma
VPP	20.23925	48.88574	Vernár – Pusté Pole	Wetterstein Dolomite	227–237	<227 Ma
GRL	19.91778	48.70361	Griľka	Wetterstein Limestone	237–242	<237 Ma
LDI	19.98222	48.70194	Lom Dielik	Wetterstein Limestone	237–242	<237 Ma
KAS	19.90556	48.69889	Kášter	Wetterstein Limestone	237–242	<237 Ma
MSE	20.03750	48.73694	Muráň – Sedlo	Wetterstein Limestone	237–242	<237 Ma
CSK	20.12972	48.81806	Červená Skala	Wetterstein Limestone	237–242	<237 Ma
REJ	19.91750	48.66556	Rejkovo	Bódvaszilas and Szin fms.	250–255	<250 Ma

Sarmatian volcanic rocks

In the study area, two sites (Lašťoky and Pod Dielom abandoned quarry) with well-outcropped Sarmatian volcanic rocks were studied (Table 1). The Lašťoky site is located 4 km NW of Tisovec on the left bank of the Rimava River (Fig. 2). The faults were measured on the forest road, mainly in the stock of biotite diorite. The Pod Dielom abandoned andesite quarry is positioned approximately 7.5 km northwest of Tisovec, close to the state road between Tisovec and Brezno (Fig. 2).

Sarmatian volcanic rocks contain faults originating in strike-slip and extensional tectonic regimes, which can be divided into three homogeneous groups (cf. Table 2; Fig. 4). Theoretically, the faults could have occurred in the time interval from the Sarmatian (11.2 Ma) to the Holocene. The youngest observed tectonic regime on fault surfaces is considered to be extensional with a W–E to NW–SE-trending principal minimal paleostress axis (σ_3) The normal faults are younger than the strike-slip faults, based on cross-cutting criteria on the outcrops. In general, the slickenside lineations on normal faults are usually without any mineral fibres (Fig. 4).

The significantly older paleostress field refers to the strike-slip tectonic regime with the orientation of maximum paleostress axis (σ_1) in a NE–SW direction, while the minimum paleostress axis (σ_3) was in a NW–SE direction. The fault-slip group is composed of N–S trending dextral and ENE–WSW trending sinistral strike-slip faults, which are considered to be a conjugate fault system (Fig. 4).

The oldest state of a paleostress field recorded in the Sarmatian volcanic rocks is characterised by an NNW–SSE trending maximal paleostress axis (σ_1) and an ENE–WSW trending minimal paleostress axis (σ_3), as well as by a strike-slip tectonic regime. On the basis of these obtained data from the volcanic rocks, the evolution of paleostress field orientation refers to the progressive rotation of the paleostress axis (σ_1) from an NNW–SSE to NE–SW position. All of the aforementioned slickenside lineations are composed of calcite, quartz, epidote, and chabazite mineral fibres. Some of them are without any mineral fill.

Upper Eocene to Oligocene sedimentary formations

The brittle structures evidenced in the Priabonian to Rupelian age are heterogeneous, and when using the paleostress determination by stress inversion, the fault-slips contain two main deformational phases that had never been observed in the Sarmatian volcanic rocks (Table 2). Of course, deformations known from the Sarmatian rocks were also observed in the sediments of the Central Carpathian Paleogene deposits. On the basis of this criterion, these phases should be considered older than the Sarmatian period and younger than the Chattian.

The deformational structures are characterised predominantly by strike-slip and extensional tectonic regimes with different orientation of the principal paleostress axes. The distinct deformational stage is represented by the strike-slip tectonic regime with the NW–SE-trending σ_1 and NE–SW-trending σ_3. In the upper Eocene to Oligocene sediments, predominantly N–S sinistral and WNW–ESE dextral faults were found. Brittle deformation represented by fault-slips is

Table 2: Paleostress tensors computed from fault-slip data. Explanations: Code – code of site, which is also used in Table 1 and Figs. 4, 5, 6; Site – name of the site; *n* – number of fault-slips used for stress tensor determination; *nT* – total number of fault data measured on a site; σ_1, σ_2, and σ_3 – azimuth and plunge of principal stress axes; *Φ* – stress ratio; *Φ'* – tensor type index as defined in the text (for further information see Delvaux et al. 1997); α – mean slip deviation (in degree).

Code	Site	*n*	*nT*	σ_1	σ_2	σ_3	*Φ*	*Φ'*	α
LAS-A	Tisovec – Lašťoky A	11	22	157/25°	313/63°	062/10°	0.32	1.68	9.2
LAS-B	Tisovec – Lašťoky B	11	22	212/13°	097/60°	308/26°	0.22	1.78	8.4
PDI-A	Tisovec – Pod Dielom quarry A	20	47	018/02°	282/70°	109/20°	0.24	1.76	11.8
PDI-B	Tisovec – Pod Dielom quarry B	7	47	334/14°	125/74°	242/08°	0.57	1.43	6.2
PDI-C	Tisovec – Pod Dielom quarry C	9	47	013/88°	103/00°	193/02°	0.19	0.19	2.7
PDI-D	Tisovec – Pod Dielom quarry D	5	47	316/70°	196/10°	103/17°	0.30	0.30	9.0
MAV-A	Tisovec – Magnet hill A	1	5	012/20°	229/65°	107/14°	–	–	0.0
MAV-B	Tisovec – Magnet hill B	4	5	233/17°	040/72°	142/04°	0.23	1.77	7.5
STO-A	Spišské Tomášovce – Ďurkovec A	13	63	353/06°	144/83°	263/04°	0.38	1.62	7.3
STO-B	Spišské Tomášovce – Ďurkovec B	21	63	024/03°	127/77°	294/12°	0.38	1.62	7.8
STO-C	Spišské Tomášovce – Ďurkovec C	6	63	101/59°	344/15°	246/26°	0.40	0.40	5.6
STO-D	Spišské Tomášovce – Ďurkovec D	4	63	001/85°	183/05°	093/00°	0.42	0.42	1.8
HRA-A	Hrabušice – Podlesok A	5	7	200/27°	061/56°	300/19°	0.57	1.43	10.2
HRA-B	Hrabušice – Podlesok B	2	7	123/01°	223/82°	033/08°	–	–	3.3
DLJ-A	Dobšinská Ľadová Jaskyňa A	4	39	208/04°	324/81°	117/08°	0.38	1.62	3.6
DLJ-B	Dobšinská Ľadová Jaskyňa B	13	39	274/10°	131/78°	005/07°	0.39	1.61	13.6
DLJ-C	Dobšinská Ľadová Jaskyňa C	2	39	222/71°	067/17°	335/08°	–	–	5.6
DLJ-D	Dobšinská Ľadová Jaskyňa D	8	39	357/24°	160/65°	264/06°	0.31	1.69	11.8
DLJ-E	Dobšinská Ľadová Jaskyňa E	5	39	120/07°	239/76°	028/12°	0.38	1.62	11.9
TIS-A	Tisovec – Dúhovo A	19	59	272/17°	066/71°	180/08°	0.56	1.44	8.7
TIS-B	Tisovec – Dúhovo B	4	59	191/04°	334/85°	100/03°	0.50	1.50	0.8
TIS-C	Tisovec – Dúhovo C	5	59	130/15°	249/61°	033/24°	0.32	1.68	8.7
TIS-D	Tisovec – Dúhovo D	3	59	001/58°	199/31°	104/08°	–	–	27.1
TIS-E	Tisovec – Dúhovo E	12	59	229/08°	016/80°	139/05°	0.39	1.61	6.3
TIS-F	Tisovec – Dúhovo F	2	59	074/57°	338/03°	246/33°	0.62	0.62	7.5
TIS-G	Tisovec – Dúhovo G	6	59	312/21°	185/58°	051/23°	0.42	1.58	13.2
TIS-H	Tisovec – Dúhovo H	2	59	354/61°	246/09°	151/27°	–	–	8.9
JAV-A	Tisovec – Javorina A	3	3	021/57°	233/29°	135/15°	–	–	29.6
CRM-A	Tisovec – Čeremošná A	15	104	278/01°	177/82°	008/08°	0.35	1.65	4.3
CRM-B	Tisovec – Čeremošná B	11	104	167/08°	052/70°	260/18°	0.50	1.50	8.5
CRM-C	Tisovec – Čeremošná C	59	104	022/83°	126/02°	216/07°	0.40	0.40	10.1
CRM-D	Tisovec – Čeremošná D	6	104	240/84°	066/06°	336/01°	0.45	0.45	10.3
CRM-E	Tisovec – Čeremošná E	5	104	022/64°	157/19°	253/17°	0.65	0.65	4.8
CRM-F	Tisovec – Čeremošná F	5	104	043/22°	313/01°	220/68°	0.73	2.73	4.2
CRM-G	Tisovec – Čeremošná G	3	104	229/30°	206/05°	108/60°	0.50	2.50	4.7
TEP-A	Tisovec – Teplica A	2	4	276/25°	080/65°	183/06°	–	–	7.6
TEP-B	Tisovec – Teplica B	4	4	051/08°	316/30°	155/59°	–	–	11.9
LPH-A	Predná Hora A	8	29	320/13°	081/66°	225/20°	0.35	1.65	7.2
LPH-B	Predná Hora B	9	29	173/28°	325/59°	077/12°	0.28	1.72	10.1
LPH-C	Predná Hora C	4	29	353/15°	144/73°	261/08°	0.50	1.50	8.6
LPH-D	Predná Hora D	5	29	222/14°	012/74°	130/08°	0.20	1.80	17.0
VKO-A	Vernár – Kopanec A	16	57	253/07°	128/77°	345/10°	0.79	1.21	16.2
VKO-B	Vernár – Kopanec B	11	57	153/23°	336/67°	243/01°	0.56	1.44	10.8
VKO-C	Vernár – Kopanec C	9	57	023/05°	233/85°	113/03°	0.63	1.37	8.1
VKO-D	Vernár – Kopanec D	8	57	120/29°	305/61°	211/02°	0.60	1.40	12.8
VKO-E	Vernár – Kopanec E	8	57	268/72°	060/16°	152/08°	0.60	0.60	6.1
MLH-A	Muráň – Pod hradom A	13	46	123/03°	032/15°	224/75°	0.31	1.69	16.8
MLH-B	Muráň – Pod hradom B	11	46	173/18°	028/69°	267/11°	0.29	1.71	18.3
MLH-C	Muráň – Pod hradom C	5	46	192/33°	021/57°	285/04°	0.50	1.50	11.3
MLH-D	Muráň – Pod hradom D	4	46	232/18°	083/69°	326/10°	0.69	1.31	1.3
MLH-E	Muráň – Pod hradom E	6	46	344/05°	075/09°	225/80°	0.24	2.24	4.8
MLH-F	Muráň – Pod hradom F	5	46	317/85°	214/01°	124/05°	0.63	0.63	10.9
MLH-G	Muráň – Pod hradom G	2	46	280/78°	111/12°	021/02°	–	–	22.3
LNO-A	Muráň – Lom nad obcou A	6	13	241/81°	344/02°	075/09°	0.36	0.36	3.1
LNO-B	Muráň – Lom nad obcou B	2	13	177/82°	311/05°	041/05°	–	–	12.0
LNO-C	Muráň – Lom nad obcou C	1	13	027/17°	125/24°	265/60°	–	–	0.0
GRU-A	Tisovec – Grúniky A	7	7	323/21°	111/66°	228/12°	0.61	1.39	16.8

Table 2 (continued)

Code	Site	*n*	*nT*	σ_1	σ_2	σ_3	*Φ*	*Φ'*	*α*
VPP-A	Vernár – Pusté Pole A	13	121	038/79°	231/11°	140/02°	0.22	0.22	17.3
VPP-B	Vernár – Pusté Pole B	37	121	018/14°	221/74°	110/06°	0.44	1.56	10.0
VPP-C	Vernár – Pusté Pole C	21	121	048/16°	235/73°	138/02°	0.39	1.61	12.6
VPP-D	Vernár – Pusté Pole D	22	121	132/01°	038/73°	222/17°	0.36	1.64	9.4
VPP-E	Vernár – Pusté Pole E	6	121	159/16°	318/73°	067/06°	0.45	1.55	7.4
VPP-F	Vernár – Pusté Pole F	11	121	261/20°	046/66°	167/13°	0.69	1.31	13.7
VPP-G	Vernár – Pusté Pole G	2	121	062/59°	317/09°	222/30°	0.50	0.50	8.6
GRL-A	Tisovec – Griľka A	22	125	265/14°	147/62°	001/24°	0.50	1.50	13.3
GRL-B	Tisovec – Griľka B	14	125	124/10°	258/76°	032/10°	0.55	1.45	16.5
GRL-C	Tisovec – Griľka C	13	125	324/26°	180/58°	062/16°	0.50	1.50	12.1
GRL-D	Tisovec – Griľka D	14	125	353/75°	184/15°	093/03°	0.26	0.26	12.5
GRL-E	Tisovec – Griľka E	17	125	040/07°	141/57°	305/32°	0.22	1.78	9.6
GRL-F	Tisovec – Griľka F	12	125	359/82°	119/04°	209/06°	0.59	0.59	5.9
GRL-G	Tisovec – Griľka G	5	125	069/69°	257/21°	166/03°	–	–	5.4
LDI-A	Tisovec – Lom Dielik A	4	8	271/78°	104/11°	014/03°	0.35	0.35	6.2
LDI-B	Tisovec – Lom Dielik B	4	8	112/45°	340/34°	231/26°	0.29	0.29	12.1
KAS-A	Tisovec – Kášter A	3	8	095/13°	237/73°	003/10°	–	–	4.0
KAS-B	Tisovec – Kášter B	2	8	350/18°	128/67°	255/15°	–	–	22.0
KAS-C	Tisovec – Kášter C	3	8	022/71°	220/18°	128/05°	–	–	50.3
MSE-A	Muráň – Saddle A	7	14	199/34°	012/55°	107/03°	0.13	1.87	7.8
MSE-B	Muráň – Saddle B	2	14	332/81°	241/00°	151/09°	–	–	9.6
MSE-C	Muráň – Saddle C	4	14	189/10°	098/04°	349/79°	0.23	2.23	3.0
MSE-D	Muráň – Saddle D	1	14	106/26°	242/56°	006/21°	–	–	0.0
CSK-A	Šumiac – Červená Skala A	5	8	140/16°	026/56°	239/30°	0.72	1.28	11.1
CSK-B	Šumiac – Červená Skala B	1	8	248/34°	344/09°	086/55°	–	–	0.0
CSK-C	Šumiac – Červená Skala C	2	8	304/12°	109/78°	213/03°	–	–	0.6
REJ-A	Tisovec – Rejkovo A	1	9	336/09°	081/57°	240/32°	–	–	0.0
REJ-B	Tisovec – Rejkovo B	8	9	008/07°	119/71°	275/17°	0.41	1.59	10.5

well-preserved in the Priabonian deposits of the Borové Formation at the locality of the Ďurkovec quarry (Fig. 6).

The younger, extensional tectonic regime is depicted by the generally NE–SW oriented σ_3 paleostress axis, while the principal compressional paleostress axis σ_1 remains subvertical. The pure extension was responsible for the evolution of the NW–SE striking on both sides of the moderately to steeply-dipping normal and oblique faults (Fig. 5).

The homogeneous fault-slips of the mainly strike-slip kinematics underwent a strike-slip tectonic regime with the generally N–S-oriented σ_1 and W–E-oriented σ_3 (Fig. 5). The NW–SE dextral and NE–SW sinistral trending strike-slip faults dominate at many sites (e.g., Ďurkovec quarry, etc.). Significantly different strike-slip tectonics with the NE–SW-trending paleostress axis σ_1 and NW–SE-trending paleostress axis σ_3 was also evidenced in the upper Eocene to Oligocene sediments of the Central Carpathian Paleogene Basin. During this paleostress field pattern, the N–S dextral and E–W sinistral strike-slip faults were predominantly active on weakness planes. These paleostress fields belong to the late Neogene Period.

Upper Cretaceous sedimentary formations and crystalline basement

The Upper Cretaceous formation has been preserved only in isolated denudation relics (Fig. 2). Occurrences around the Dobšinská Ľadová Jaskyňa settlement are the second largest in the Central Western Carpathians after the Myjava Uplands (Brezová Group). The only suitable locality for measuring the brittle deformations in these sediments is an outcrop in the Červená Skala–Margecany railway, which is cut close to the Dobšinská Ľadová Jaskyňa railway station (Table 2). The rocks were relatively rich in fault structures, very often with a distinctly-definable direction and sense (orientation) of movement. In essence, the kinematics of the fault-slip was clearly determinable based on the mineral accretional steps of calcite fibres.

The second group of rock is composed of metagranitoids, schists, gneisses, metaquartzites and marbles of the Veporic Unit in the broader area of the town of Tisovec, which underwent the Alpine metamorphosis in greenschist to amphibolite facies during the Late Cretaceous (≈120–85 Ma). Thus, all of the observed and measured fault-slip data are certainly younger than the Alpine metamorphosis. The slickenside lineations have been less well-preserved with quartz, calcite, hematite, and epidote-zoisite fibres in Paleo-Alpine metamorphosed rocks.

Both the Upper Cretaceous and crystalline basement/cover rocks contain all tectonic phases that were described in previous subsections, and so we will not repeat them again (Table 2). However, it is important to note that tectonic phases were also recorded in these rocks, which are absent in younger rocks. Therefore, it is possible to divide two groups of homogeneous deformational structures.

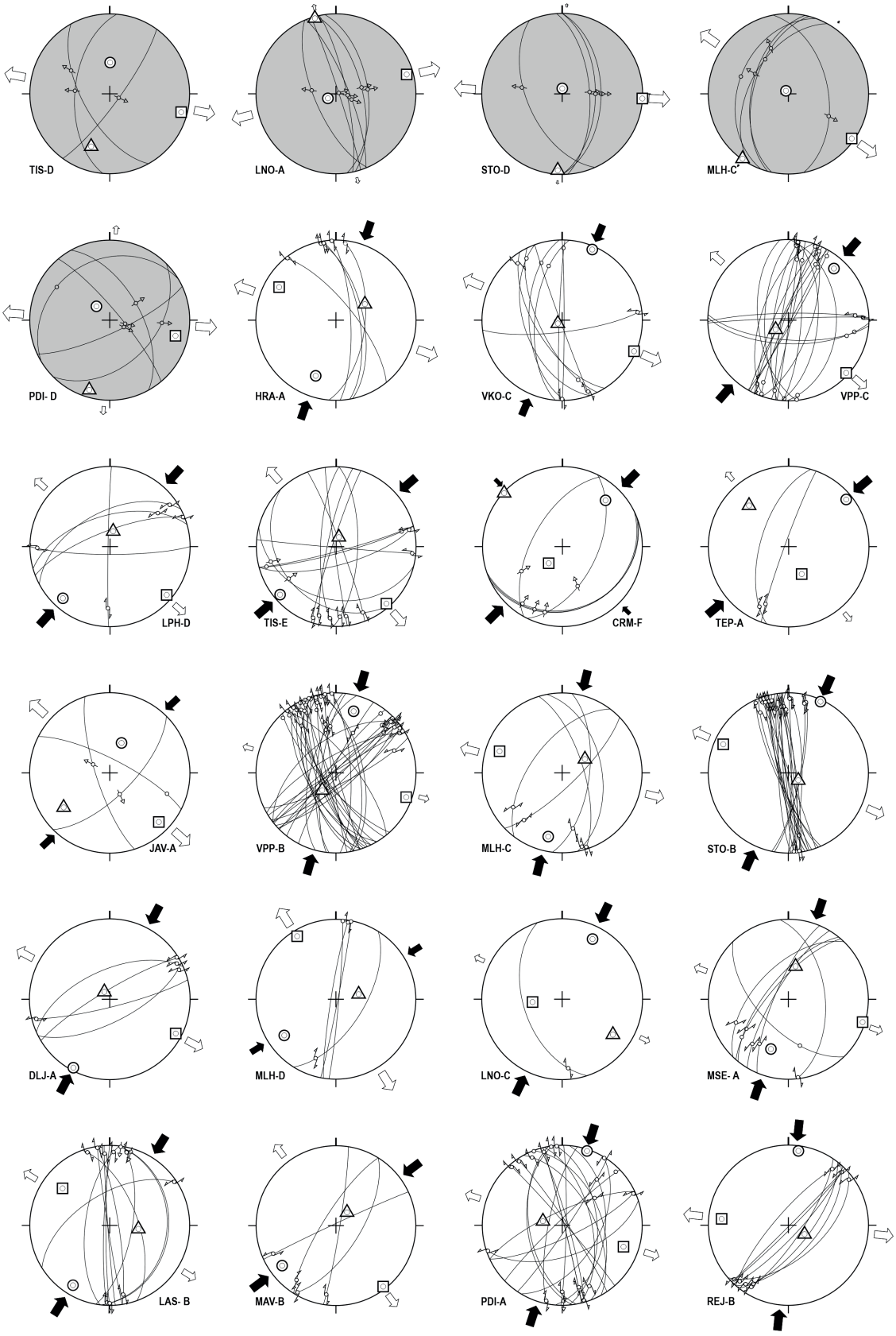

Fig. 4. Stereogram of Pannonnian to Quaternary fault-slip data. Note: grey stereograms represent Quaternary and white stereograms represent the Pannonian to Pliocene paleostress fields; circle – principal compressional paleostress axis σ_1; triangle – intermediate paleostress axis σ_2; square – principal tensional paleostress axis σ_3.

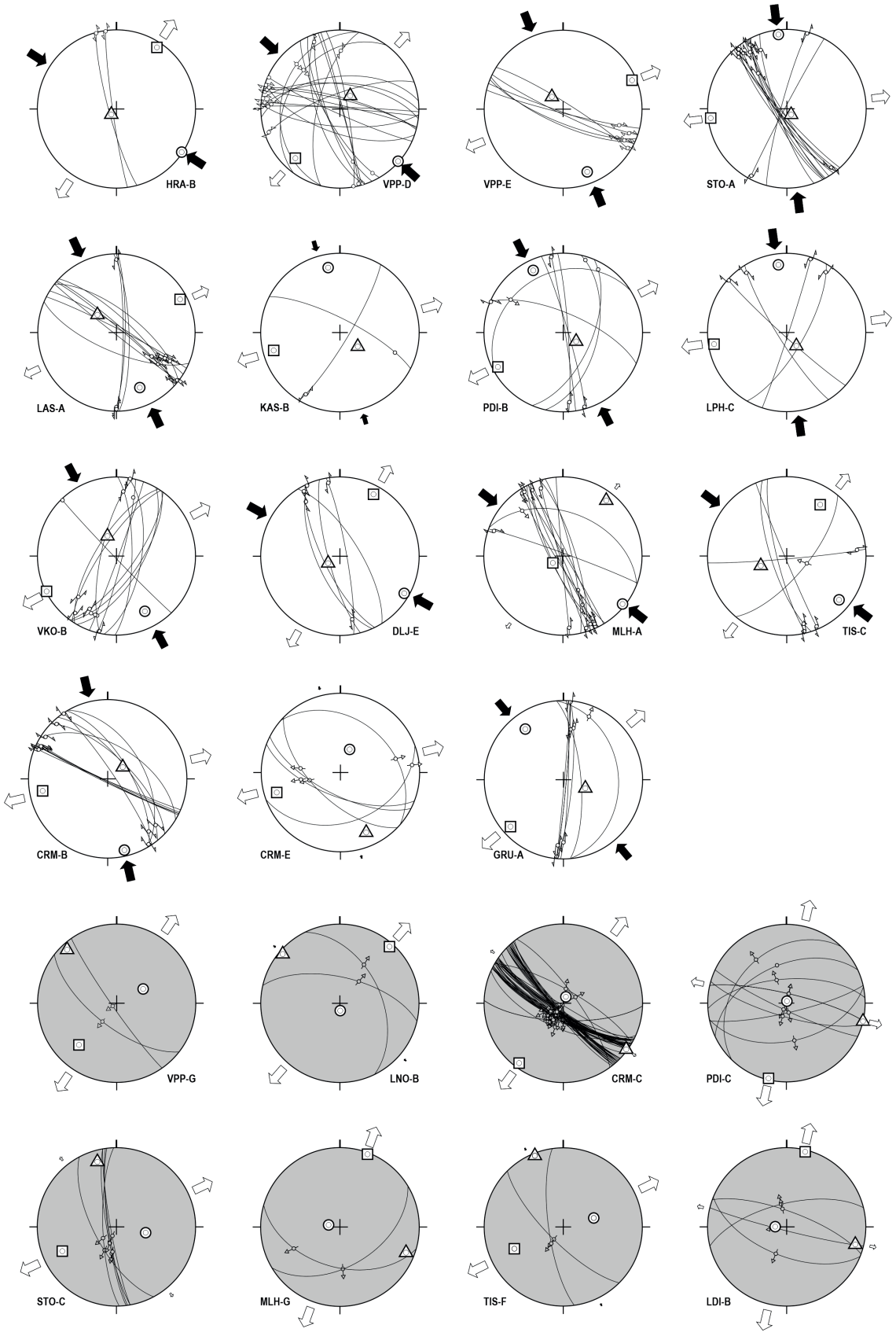

Fig. 5. Stereogram of Badenian–Pannonian fault-slip data. Note: white stereograms represent Sarmatian–Pannonian and grey stereograms represent the Badenian–Sarmatian paleostress fields.

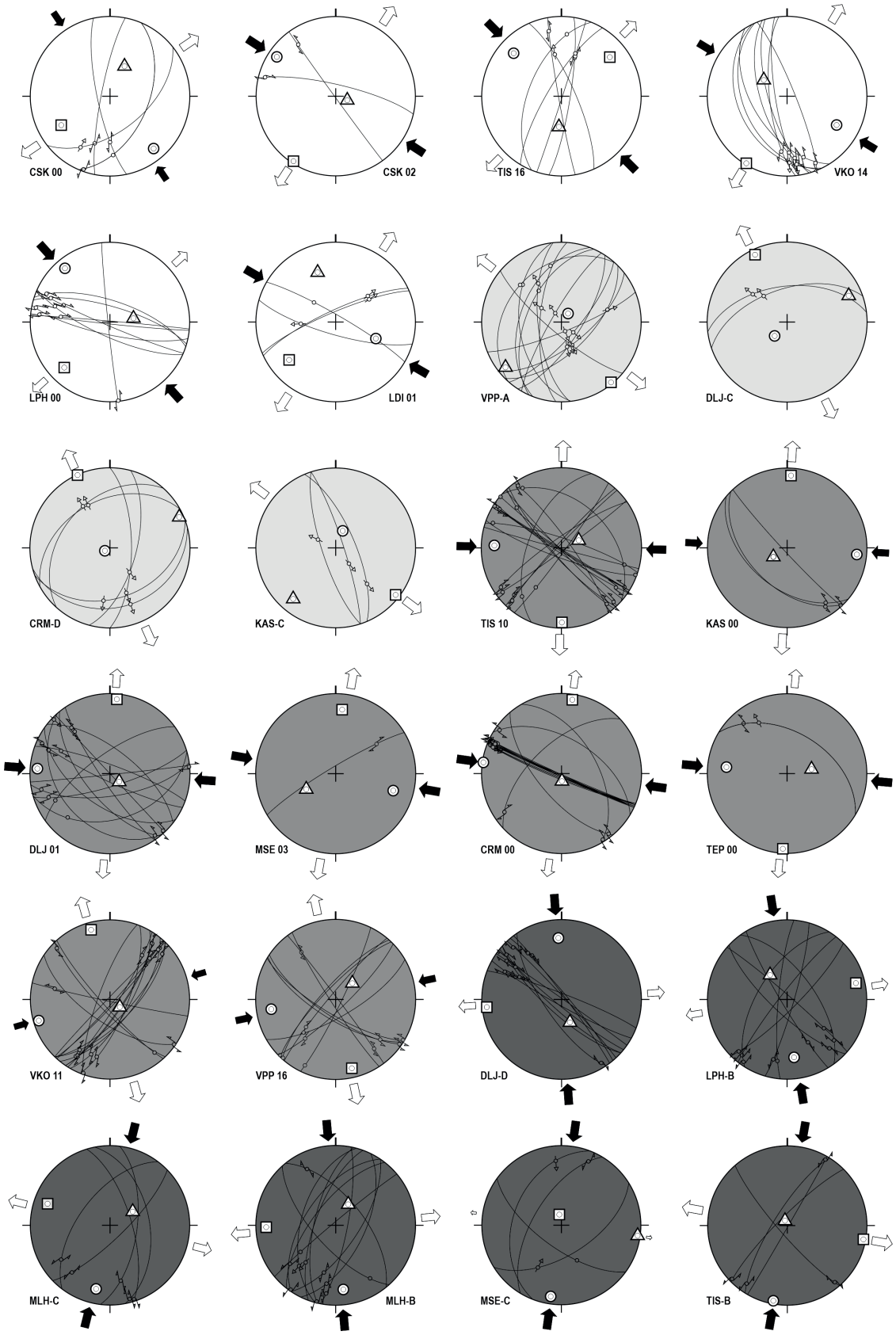

Fig. 6. Stereograms of Late Cretaceous to early Neogene fault-slip data. Note: white stereograms represent the early Neogene, light grey stereograms represent the late Eocene to Oligocene, grey stereograms represent the late Paleocene to early Eocene, and dark grey stereograms represent the Late Cretaceous paleostress fields.

The younger one is related to the strike-slip tectonic regime with the W–E-trending σ_1 and N–S-trending σ_3, and it was observed on sites with crystalline basement and Upper Cretaceous deposits. This phase is less frequently recorded in outcrops because it is overprinted by younger deformation on weakness planes. NW–SE trending sinistral and NE–SW trending dextral conjugate faults are typical structures observed and measured in the outcrops containing the Upper Cretaceous deposits or crystalline basement belonging to the Veporic Unit. The deformation finished by extension with NW–SE-trending σ_3 axis. (Fig. 6).

Chronologically older, strike-slip tectonic regime with the orientation of principal maximal paleostress axis σ_1 in N–S direction and principal minimal paleostress axis σ_3 perpendicular to it was observed. Observed structures are ductile to semiductile with evolution of meso- to large-scale fold structure in the nappe system of the Silicic Unit (Fig. 6). During this deformation, horse-tailed structures were formed in the northeast and southwest end of the Muráň fault close to Tisovec town (Figs. 2, 3).

Triassic sedimentary formations

This group includes sites that were located in unmetamorphosed Mesozoic, substantially Triassic complexes belonging to large bodies of the Vernár and Muráň nappes (Table 1). The superficial nappes exceeded only the diagenesis and approximate temperatures from the interval of 150–250 °C, which were calculated from the illite crystallinity index KI (Milovský et al. 2003). This circumstance makes it difficult to define individual tectonic phases and assign them to age, since the deformations in the nappe could have taken place at any time from the Triassic epoch up to the present. In the Triassic carbonates of the Muráň and Vernár nappes, it is possible to observe all of the aforementioned deformation phases recorded in the previous rock complexes, which are related to the evolution of the Muráň nappe (Table 2; Figs. 4–6).

Chronology of faulting – interpretation and discussion

General characteristics

The trace of the Muráň fault is highly visible in the area between Tisovec and Telgárt, which borders a NE–SW elongated segment of the Muráň superficial nappe system with respect to the Veporic crystalline basement. The fault also dislocates the Vernár and Stratená nappes and is roughly limited by the southern margin of the Hornád depression belonging to the Central Carpathian Paleogene Basin – the course of its structures through the Eocene and Oligocene deposits is poorly visible or so far unknown. The Stratená nappe system has been deformed by moderately north-dipping ENE–WSW reverse faults and by a system of synclines and anticlines, which are dislocated by the Muráň fault. Towards the southwest, the Stratená nappe disappears on the Muráň fault boundary NE of the village of Telgárt. Moreover, the Vernár nappe narrows strikingly north-eastward, passing into the narrow Betlanovce bend and is disrupted in the southwest by a NW–SE striking fault in the upper reach of the Hnilec River (Fig. 2).

The synclines and anticlines in the Muráň nappe are limited in the SE by the Muráň fault (cf. Bystrický 1959; Vojtko 2000; Pelech & Kronome 2019). The fault is accompanied by a set of parallel dislocations, which produced the tectonic slices and klippen-like structures in the area of Telgárt and Tisovec. The klippes are composed of the Middle to Upper Triassic carbonates, while the klippen mantle is formed exclusively by upper Permian to Lower Triassic siliciclastic deposits. The syncline of the Muráň nappe strikingly narrows north-eastwards into the narrow Telgárt bend. In the southwest, approximately 4.5 km from Tisovec, the Muráň nappe disappears, and the continuation of the Muráň fault inside the Veporic crystalline basement is less visible also due to an overstepping structure (Fig. 2).

Campanian to Bartonian evolution (~80–38 Ma)

The time span between the Campanian and Danian represents tectonic phases, which occur immediately after the unroofing the Veporic metamorphic dome and the deposition of the Gosau Group deposits (e.g., Madarás et al. 1996; Plašienka et al. 2007; Jeřábek et al. 2008, 2012; Králiková et al. 2016; Vojtko et al. 2016). The unroofing of the Veporic dome from beneath the Gemeric Unit and the Meliata nappe stack took place later than the Alpine metamorphic maximum and earlier than emplacement of the Rochovce granite intrusion. The peak of the Paleo-Alpine metamorphism in the Veporic Unit may be as old as 115 Ma as recorded by $^{40}Ar/^{39}Ar$ and K–Ar ages (Kováčik et al. 1996, 1997; Maluski et al. 1993) and Sm–Nd whole rock-garnet isochron (108.8±5.6 Ma; Lupták et al. 2004). The lateral orogen-parallel extension of the Veporic Unit finished at the latest by 97±4 Ma, which is suggested by the post-kinematic growth of monazite in the southern Veporic cover sequences dated by the laser ablation ICP-MS method (Bukovská et al. 2013). The subsurface Cretaceous Rochovce granite occurring in the close proximity to the Lubeník thrust zone and revealing U–Pb, Re–Os ages respectively from 76 to 82 Ma (Hraško et al. 1999; Poller et al. 2001; Kohút et al. 2013) intruded the already active sinistral transpressive zone.

Based on the aforementioned momentous data, the Muráň fault may be as old as ~85–80 Ma and originated as a ductile shear zone at mid-crustal depth, which was transformed, by gradual exhumation to a semi-ductile and brittle shear zone. During the Late Cretaceous to Paleocene, the fault can be considered a sinistral transpressional strike-slip fault under a paleostress field with the sub-horizontal orientation principal maximum paleostress axis σ_1 in ~N–S direction and a perpendicular principal minimum paleostress axis σ_3 (Figs. 6, 7). In addition to numerous measurements of strike-slip duplexes

Observed rocks / Appox. age of faulting	Triassic deposits	Veporic crystalline basement	Upper Cretaceous deposits	Upper Eocene - Lower Oligo. deposits	Tortonian volcanic rocks
Quaternary (< 2.6 Ma)	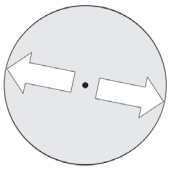	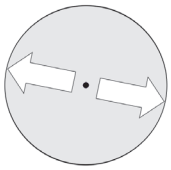		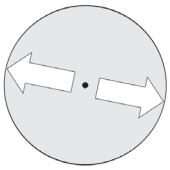	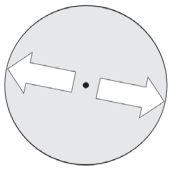
Pliocene (5.3 – 2.6 Ma)	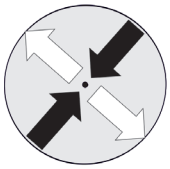	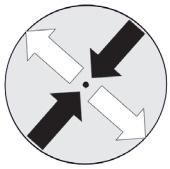	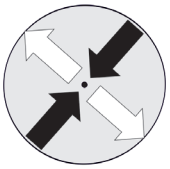	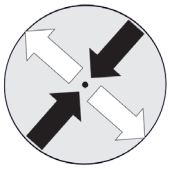	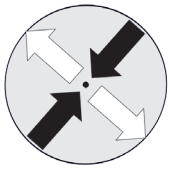
Sarmatian – Pannonian (11.2 – 5.3 Ma)	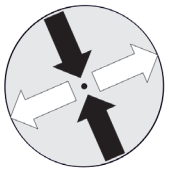	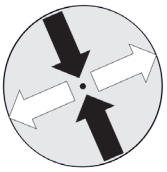	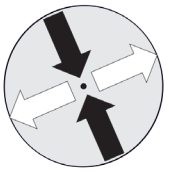	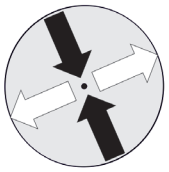	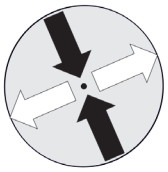
Badenian – Sarmatian (16.3 – 11.2 Ma)	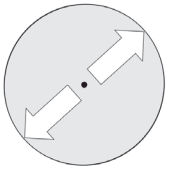	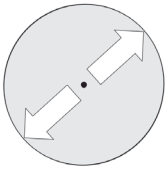		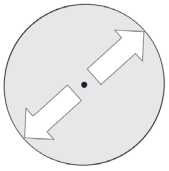	
Eggenburgian – Karpatian (21.4 – 16.3 Ma)	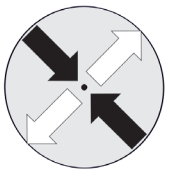	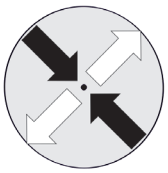	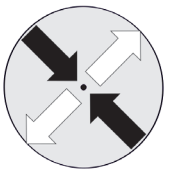	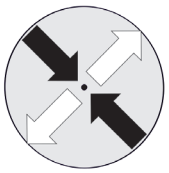	
Priabonian – Chattian (37.7 – 23.0 Ma)	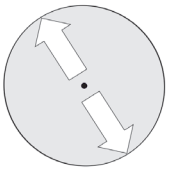	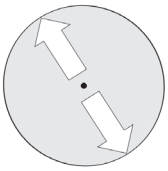	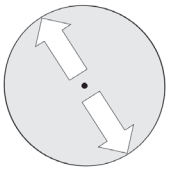		
Ypresian – Bartonian (56.0 – 37.7 Ma)	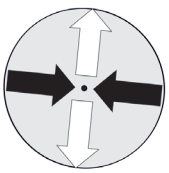	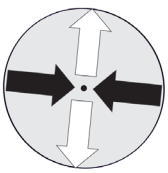	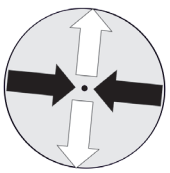		
Danian – Thanetian (66.0 – 56.0 Ma)	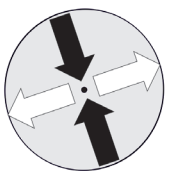	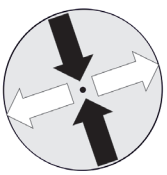	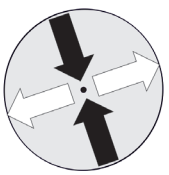		

Fig. 7. Synthetic table of chronology for the Late Cretaceous to Quaternary regional stress fields.

in the shear zone of the Muráň nappe body, several open to closed anticlines and synclines have been identified with a W–E trend of their axes (cf. Bystrický 1959; Klinec 1976; Vojtko 2000; Kronome & Bórová 2014; Pelech & Kronome 2019). The compressional tectonic regime with backthrust movement (vergence southwards) was also documented in the Northern Gemeric Unit (Vozárová 1995) and the Stratená nappe, where imbrication of a partial nappe originated (e.g., Maheľ 1957). The ENE–WSW axes of large fold structures in the Muráň nappe bend to the NE–SW direction close to the Muráň fault zone also refer to sinistral strike-slip movement on the fault. For the time being, the sinistral strike-slip motion has been conditionally deduced by previous works as well (e.g., Pospíšil et al. 1989; Marko 1993).

A significant reorganization of the paleostress field was carried out approximately at the boundary of the Paleocene and Eocene. The principal compressional paleostress axis σ_1 replaced its position from the N–S to W–E direction and the principal tensional paleostress axis σ_3 from W–E to a N–S direction (Figs. 6, 7). During this deformation, the movement on the Muráň fault changed to dextral, and the secondary fan-shaped structures in the SW part of Muráň nappe were most likely reactivated to the oblique normal fault fan formed during this time. On the other hand, the reverse faults of the Stratená nappe that had formed during the previous stage were rearranged to the fan structures, which converge in the Telgárt bend (cf. Fig. 2). These structures certainly originated after the Danian, since sediments of the Gosau Group are incorporated into these structures; however, the upper Eocene to Oligocene deposits do not (cf. Fig. 3, cross-section A–B). Thus, during this deformation, an imbricated fan structure was continuously formed in the Stratená nappe as a result of strike-slip movement at the main Muráň fault zone. The dextral-strike slip motion in the fault had to be completed before the transgression of upper Eocene deposits of the Central Carpathian Paleogene Basin at the latest. This statement is supported by numerous measurements in Oligocene sediments where no significant W–E trending shortening has ever been documented (cf. Marko et al. 1995; Pešková et al. 2009; Vojtko et al. 2010; Sůkalová et al. 2012). The strike-slip tectonic regime with the W–E-trending principal maximum paleostress axis has also been determined in previous works. Pelech & Kronome (2019) consider this deformation early Eocene. However, their work did not formulate precisely which criteria the authors had included for the determination of the deformation period. Moreover, some authors tenuously date this deformation to the Miocene period, but not younger than the Sarmatian (e.g., Marko 1993).

Priabonian to Egerian evolution (~37–21 Ma)

In the late Eocene, activity of the Muráň fault began to gradually decrease, and the fault structure is more or less sealed by the Priabonian transgressive deposits of the Hornád depression. This is pointed out by the evenly-distributed lithofacies of the Eocene and Oligocene formations in the southern part of the Hornád depression on both sides of the Muráň fault without any significant changes. These sedimentary deposits are shifted less than 100 metres by the fault (cf. Fig. 2 upper Eocene transgressive contact with respect to the Paleo-Alpine structure). In this time, the transgression was likely controlled by the extensional tectonic regime of the upper plate in the forearc position with the orientation of σ_3 in a general N–S to NE–SW direction (Figs. 6, 7). Such orientation of principal least stress axis was also determined by Pelech & Kronome (2019). The external Tatric–Fatric–Hronic nappe system of the Central Carpathian thrust sheet was submerged beneath the upper Eocene to Oligocene deposits. The process gradually led to the burial of the Veporic and Gemeric area under the Oligocene deposits as well. This is evidenced by several erosive remnants of open marine upper Eocene to Oligocene sediments preserved in different parts of the Veporic and Gemeric zones (cf. Fig. 2). Some examples include the Brezno depression, Magnet hill, and Kláštorisko (e.g., Mello et al. 2000a,b; Vojtko 2000; Plašienka & Soták 2001; Soták et al. 2005; Kováč et al. 2016). During this period, the Muráň fault was practically inactive and segmented by the NW–SE trending normal faults (cf. Fig. 2). This corresponds to the general opinion that the main activities of the Muráň fault were carried out in the pre-late Eocene epoch (cf. Maheľ et al. 1967; Marko 1993).

Egenburgian to Badenian evolution (~21–12 Ma)

This time span comprises the evolution of the paleostress field immediately after the inversion of the Central Carpathian Paleogene Basin and before the volcanic activity in the Tisovec Intrusive Complex of Sarmatian age. Sedimentation in the Central Carpathian Paleogene Basin (Hornád depression) progressively terminated by deposition of regressive facies in the early Miocene (e.g., Soták et al. 2001), which was followed by the rejuvenation of a transpressional tectonic regime with NW–SE directed σ_1. It should be noted that Pelech & Kronome (2019) also recorded a paleostress field for this time span. However, less numerous data on this deformation is available from structural observations in the study area. Strike-slip slickenside lineations were observed in the upper Eocene sediments at the Hrabušice (HRA) site (Fig. 2). It is likely that the Muráň fault was successively activated as a sinistral transpressive shear zone, and the fault fan structures in the Vernár–Stratená nappe system could be reactivated as reverse or oblique reverse faults (Figs. 6, 7). However, this assumption is not easy to confirm, and it seems that the movements of the fault structures related to the Muráň fault system were only minimal and affected the geological structure in the area only slightly during the early and middle Miocene. This transpressional tectonic regime is likely related to the collision of the ALCAPA Mega-Unit with the European Platform in the External Western Carpathians (e.g., Kováč et al. 2017).

Conversely, the study area was controlled by an extensional tectonic regime with the NE–SW-trending principal minimal paleostress axis σ_3 in the middle Miocene period (Badenian;

Figs. 5, 7). The extension caused significant movements in some faults, which consequently led to substantial normal faulting. Along the NW–SE-striking Tisovec fault, the downthrown block movement was significant with a magnitude of more than 750 m (cf. Pulec 1966; Marko & Vojtko 2006). The movement along the Tisovec fault is confirmed by preserved Oligocene sediments in the hanging wall (Brezno Basin and Magnet hill (Fig. 2). Moreover, the Muráň fault is dissected by NW–SE-striking faults in several places (e.g., the town of Tisovec, Predná hora, and the Pusté Pole passes) and originated during this time span.

Sarmatian to recent evolution (~12 Ma to Holocene)

The period between the Sarmatian to Quaternary was controlled by three different paleostress fields, which were identified in the Sarmatian andesite subvolcanic bodies, diorite intrusions (Figs. 4, 5, 7), and Pleistocene travertine (Sůkalová et al. 2012). The principal compressional axis σ_1 rotated from the NNW–SSE to the NE–SW position from Sarmatian to Pliocene. The Sarmatian(?) paleostress field can be characterised by NNW–SSE trending σ_1 and WNW–ESE trending σ_3 in a strike-slip tectonic regime (Figs. 5, 7). The orientation of the paleostress field allows for tectonic movement of the Muráň fault in a left-lateral strike-slip motion.

The more dominant, however, is the Pliocene(?) strike-slip tectonic regime with the NE–SW oriented σ_1 compressional paleostress axis and NW–SE directed σ_3 extensional one (Figs. 4, 7). The relationship of these structures was clearly evidenced using cross-cutting criteria. Such orientation of the paleostress field did not allow for strike-slip movement of the Muráň fault. At the end of the strike-slip tectonic regime, transtension was replaced by extension.

Neotectonic movements in the study area are difficult to identify, since it is a problem to filter out from older faults. This is mainly because rocks younger than Miocene volcanics (Sarmatian) do not occur in the area, except for Quaternary slope debris, terrace, and alluvial deposits. The absence of upper Miocene and Pliocene sediments greatly increases the uncertainty of the dating of the youngest tectonic events. However, during the Pliocene–Quaternary, the Muráň fault was tenuously activated as a normal fault, and its motion was controlled by extensional tectonic regime with the WNW–ESE to NW–SE oriented principal minimal stress axis σ_3 (Figs. 4, 7). The extensive tectonic regime probably persisted throughout the neotectonic period. This is supported by measurements of deformation of structures in the lower Pleistocene travertine body of the Hranovnické pleso (cf. Sůkalová et al. 2012) and different distribution of thickness of fluvial deposits in the Rimava and Muráň rivers fluvial plane. Quaternary alluvial deposits on the NW downthrown block reach a thickness of more than 12 meters; however, in most cases, the deposits are practically missing or very thin in the SE upthrown block (less than 2 meters). The NW block was downthrown at least 10 m against the SE block. This finding is confirmed by drilling works in the urban areas of Tisovec and Muráň (e.g., Vojtko 2003). In addition, the well-consolidated Pleistocene carbonate Muráň breccia (Ložek 1960) is deformed by the Muráň fault, as well as its synthetic structures in the Muráň pod Hradom site (cf. Putiška et al. 2012).

Conclusions

The study area, where the Muráň fault is outcropped, is composed of the Paleo-Alpine tectonic units that are divided to the stack of basement-dominated nappes and superficial thrust sheets. The first group contains the north-verging, thick-skinned Veporic and Gemeric basement/cover thrust sheets and the second one is dominated by the Jurassic Muráň–Vernár–Stratená nappe system belonging to the Silicic Unit reactivated during the Cretaceous. The nappe stack is roughly sealed by post-nappe cover formations, which are represented by sedimentary succession of the Central Carpathian Paleogene Basin. The Upper Cretaceous deposits have a specific transitional position with respect to the nappe structure.

Structural measurements were carried out predominantly in abandoned quarries, outcrops along roads, railways, and on cliffs as well. Based on the fault-slip analysis, the strike-slip kinematics play a substantial role in the evolution of the Muráň fault zone. The Muráň fault may be as old as ~85–80 Ma and can be considered a sinistral transpressional strike-slip fault with imbrication of a partial nappe that originated during the Late Cretaceous to Paleocene. A significant reorganization of the paleostress field was carried out approximately at the boundary of the Paleocene and Eocene, and the movement on the Muráň fault changed to dextral. In this time span, secondary fan-shaped structures along the fault were formed. Based on the lithostratigraphic and structural criteria, the structures originated after the Danian and completed before the late Eocene.

The Neogene evolution of the fault is characterised by continuous change of the orientation of paleostress field and the fault started to become sinistral transpressional to transtensional up to a normal fault. However, the movement along the fault was only several tens of metres. The fault movement was practically negligible compared to the previous Late Cretaceous to early Eocene period. The Neotectonic phase (Pliocene–Holocene) is characterised by extensional a tectonic regime with the orientation of principal least axis σ_3 in a WNW–ESE direction, and normal faulting is indicated by borehole data in the alluvial planes of the Rimava and Muráň rivers.

Based on the lithostratigraphic constraints, regional geology, and chronology of Alpine metamorphic processes, it is possible to constrain the time span of fault activity of the Muráň fault. Therefore, we can declare that the main faulting took place from the latest Cretaceous to early Eocene as a ductile, and later as a brittle shear zone inside the Veporic crystalline basement.

Finally, as a Neogene structure, the Muráň fault practically did not exist, or was at least insignificant with a maximum

movement of approximately of 150 meters. Its main role was in the period from ~80 Ma to 45 Ma. The fault looks quite attractive and "active" on geological maps, satellite shots, as well as in digital elevation models, but this is simply an interplay of circumstances, especially with high contrast in the rheology of carbonate and metamorphic rocks. However, we cannot associate this fault with any important fault of Neogene in age (such as the Rába fault, etc.). Interpretation is based on numerous field observations and does not address its true significance. It is absurd that such a significant fault has never been so comprehensively processed or published in research periodicals before and has been used for various misleading interpretations without any data or arguments. We firmly believe that this article will contribute to the understanding of the tectonic evolution of the Muráň fault and the Western Carpathian orogen as well.

Acknowledgments: This paper is based on the main part of the PhD thesis undertaken during the years 1999–2004 by R.V. and 2017–2022 by S.G. Our work was supported by the Slovak Research and Development Agency under contracts No. APVV-17-0170 "Early Alpidic tectonic evolution and palaeogeography of the Western Carpathians", by the VEGA project 1/0346/20 "Central Slovak Fault System – its role during the tectonic evolution of intramontane basins and neovolcanites" and UK Grant: UK/357/2021 "Štruktúrna a biostratigrafická analýza triasových sekvencií vernárskeho príkrovu". Lászlo Fodor and Zoltán Németh are thanked for constructive reviews, which were helpful in improving this article.

References

Andrusov D., Bystrický J. & Fusán O. 1973: Outline of the structure of the West Carpathians. Guide Book, X Congress CBGA. *D. Štúr Institute of Geology*, Bratislava.

Angelier J. 1975: Sur l'analyse de mesures recueillies dans des sites faillés: l'utilité d'une confrontation entre les méthodes dynamiques et cinématiques. *Comptes rendus de l'Académie des Sciences Paris* D281, 1805–1808.

Angelier J. 1979: Determination of the mean principal directions of stress for a given fault population. *Tectonophysics* 56, T17–T26. https://doi.org/10.1016/0040-1951(79)90081-7

Angelier J. 1984: Tectonic analysis of fault slip data sets. *Journal of Geophysical Research* 89, 5835–5848. https://doi.org/10.1029/JB089iB07p05835

Angelier J. 1989: From orientation to magnitudes in paleostress determinations using fault slip data. *Journal of Structural Geology* 11, 37–50. https://doi.org/10.1016/0191-8141(89)90034-5

Angelier J. 1990: Inversion of field data in fault tectonics to obtain the regional stress – III. A new rapid direct inversion method by analytical means. *Geophysical Journal International* 103, 363–376. https://doi.org/10.1111/j.1365-246X.1990.tb01777.x

Angelier J. 1994: Fault slip analysis and palaeostress reconstruction. In: Hancock P.L. (Ed.): Continental deformation. *Pergamon Press, University of Bristol*, London, 53–100.

Angelier J. & Mechler P. 1977: Sur une méthode graphigue de recherché des contraintes principles également utilisable en tectonique et en séismologie: la méthode des diedres droits. *Bulletin de la Société géologique de France* 19, 1309–1318. https://doi.org/10.2113/gssgfbull.S7-XIX.6.1309

Angelier J., Tarantola A., Valette B. & Manoussis S. 1982: Inversion of field data in fault tectonics to obtain the regional stress – I. Single phase fault populations: a new method of computing the stress tensor. *Geophysical Journal of the Royal Astronomical Society* 69, 607–621. https://doi.org/10.1111/j.1365-246X.1982.tb02766.x

Armijo R. & Cisternas A. 1978: Un problème inverse en microtectonique cassante. *Comptes Rendus de l'Académie des Sciences Paris* D 287, 595–598.

Bacsó Z. 1964: Post-Triassic scarn deposits near Tisovec [Protriasové skarnové ložiská pri Tisovci]. *Geologické Práce*, *Zprávy* 31, 13–45 (in Slovak).

Bezák V., Biely A., Polák M., Hraško Ľ., Kohút M. & Konečný V. 2008: General geological map of the Slovak Republic (1:200 000), Map sheet 36 – Banská Bystrica. *Ministry of Environment of the Slovak Republic*, *State Geological Institute of Dionýz Štúr*, Bratislava.

Biely A., Bezák V., Elečko M., Kaličiak M., Konečný V., Lexa J., Mello J., Nemčok J., Potfaj M., Rakús M., Vass D., Vozár J. & Vozárová A. (Eds.) 1996: Geological map of Slovakia. *Ministerstvo životného prostredia SR*, *Geologická služba SR*, Bratislava.

Bott M.H.P. 1959: The mechanics of oblique slip faulting. *Geological Magazine* 96, 109–117. https://doi.org/10.1017/S0016756800059987

Broska I. & Kubiš M. 2018: Accessory minerals and evolution of tin-bearing S-type granites in the western segment of the Gemeric Unit (Western Carpathians). *Geologica Carpathica* 69, 483–497. https://doi.org/10.1515/geoca-2018-0028

Bukovská Z., Jeřábek P., Lexa O., Konopásek J., Janák M. & Košler J. 2013: Kinematically unrelated C–S fabrics: an example of extensional shear band cleavage from the Veporic Unit (Western Carpathians). *Geologica Carpathica* 64, 103–116. https://doi.org/10.2478/geoca-2013-0007

Bystrický J. 1959: Contribution to the stratigraphy of the Muráň Mesozoic (Muran Plateau) [Príspevok k stratigrafii Muránskeho mezozoika (Muránska plošina)]. *Geologické Práce*, *Zošit* 56, 1–53 (in Slovak).

Carey E. & Brunier R. 1974: Analyse théorique et numérique d'un modèle mécanique élémentaire appliqué a l'étude d'une population de failles. *Comptes rendus de l'Académie des Sciences Paris* D 279, 891–894.

Célérier B. 1988: How much does slip on reactivated fault plane constrain the stress tensor? *Tectonics* 7, 1257–1278. https://doi.org/10.1029/TC007i006p01257

Célérier B., Etchecopar A., Bergerat F., Vergely P., Arthaud F. & Laurent P. 2012: Inferring stress from faulting: from early concepts to inverse methods, *Tectonophysics* 581, 206–219. https://doi.org/10.1016/j.tecto.2012.02.009

Delvaux D.F. 1993: The TENSOR program for palaeostress reconstruction: examples from the east African and the Baikal rift zones. *Terra Nova* 5, suppl. 1, Proceedings of EUG VII, Strasbourg, 4–8 April., 1–216. https://doi.org/10.1111/j.1365-3121.1993.tb00218.x

Delvaux D. & Sperner B. 2003: New aspects of tectonic stress inversion with reference to the TENSOR program. In: Nieuwland D.A. (Ed.): New insights into structural interpretation and modelling. *Geological Society London, Special Publications* 212, 75–100. https://doi.org/10.1144/GSL.SP.2003.212.01.06

Delvaux D., Moyes R., Stapel G., Petit C., Levi K., Miroshnichenko A., Ruzhich V. & Sankov V. 1997: Paleostress reconstructions and geodynamics of the Baikal region, Central Asia. Part 2. Cenozoic rifting. *Tectonophysics* 282, 1–38. https://doi.org/10.1016/S0040-1951(97)00210-2

Demko R. & Hraško Ľ. 2013: Rhyolite body Gregová near the Telgárt village (Western Carpathians). *Mineralia Slovaca* 45, 161–174 (in Slovak with English summary).

Etchecopar A. Vasseur G. & Daignieres M. 1981: An inverse problem in microtectonics for the determination of stress tensor from fault striation analysis. *Journal of Structural Geology* 3, 51–65. https://doi.org/10.1016/0191-8141(81)90056-0

Faryad S.W. 1990: Gneiss-amphibolite complex of Gemericum. *Mineralia Slovaca* 22, 303–318 (in Slovak).

Faryad S.W. & Bernhardt H.J. 1996: Taramite-bearing metabasites from Rakovec (Gemeric Unit, the Western Carpathians). *Geologica Carpathica* 47, 349–357.

Gawlick H.-J. & Missoni S. 2015: Middle Triassic radiolarite pebbles in the Middle Jurassic Hallstatt Mélange of the Eastern Alps: implications for Triassic–Jurassic geodynamic and paleogeographic reconstructions of the western Tethyan realm. *Facies* 61, 13. https://doi.org/10.1007/s10347-015-0439-3

Gawlick H.-J., Frisch W., Vecsei A., Steiger T. & Böhm F. 1999: The change from rifting to thrusting in the Northern Calcareous Alps as recorded in Jurassic sediments. *Geologische Rundschau* 87, 644–657. https://doi.org/10.1007/s005310050237

Gephart J.W. & Forsyth D.W. 1984: An improved method for determining the regional stress tensor using earthquake focal mechanism data: an application to the San Fernando earthquake sequence. *Journal of Geophysical Research* B89, 9305–9320. https://doi.org/10.1029/JB089iB11p09305

Gross P., Köhler E. & Samuel O. 1984: A new lithostratigraphical division of the Inner-Carpathian Paleogene. *Geologické Práce, Správy* 81, 103–117 (in Slovak).

Hancock P.L. 1985: Brittle microtectonics: principles and practice. *Journal of Structural Geology* 7, 437–457. https://doi.org/10.1016/0191-8141(85)90048-3

Hancock P.L. & Barka A.A. 1987: Kinematic indicators on active normal faults in western Turkey. *Journal of Structural Geology* 9, 573–584. https://doi.org/10.1016/0191-8141(87)90142-8

Havrila M. & Ožvoldová L. 1996: Meliaticum in the Stratenská hornatina Hills. *Slovak Geological Magazine* 3–4, 335–339.

Hók J. & Hraško L. 1990: Deformation analysis of the western part of the Pohorelá line. *Mineralia Slovaca* 22, 1, 69–80 (in Slovak).

Hók J. & Vojtko R. 2011: Continuation of the Pohorelá line in pre-Cenozoic basement of the Central Slovakia Volcanic Field (Western Carpathians). *Acta Geologica Slovaca* 3, 13–19 (in Slovak with English summary).

Hók J., Kováč P. & Rakús M. 1995: Structural investigations of the Inner Carpathians: Results and interpretation. *Mineralia Slovaca* 27, 231–235.

Hovorka D., Ivan P., Mock R., Rozložník L. & Spišiak J. 1990: Sediments of Gossau type near the Dobšiná Ice Cave: ideas for their non-traditional interpretation. *Mineralia Slovaca* 22, 519–525 (in Slovak).

Hraško Ľ., Határ J., Huhma H., Mäntäri I., Michalko J. & Vaasjoki M. 1999: U/Pb zircon dating of the Upper Cretaceous granite (Rochovce type) in the Western Carpathians. *Krystalinikum* 25, 163–171.

Janák M., Plašienka D., Frey M., Cosca M., Schmidt S.T., Lupták B. & Méres Š. 2001: Cretaceous evolution of a metamorphic core complex, the Veporic unit, Western Carpathians (Slovakia): P–T conditions and in situ Ar-40/Ar-39 UV laser probe dating of metapelites. *Journal of Metamorphic Geology* 19, 197–216. https://doi.org/10.1046/j.0263-4929.2000.00304.x

Jeřábek P., Faryad W.S., Schulmann K., Lexa O. & Tajčmanová L. 2008: Alpine burial and heterogeneous exhumation of Variscan crust in the West Carpathians: insight from termodynamic and argon diffusion modelling. *Journal of Geological Society* 165, 479–498. https://doi.org/10.1144/0016-76492006-165

Jeřábek P., Lexa O., Schulmann K. & Plašienka D. 2012: Inverse ductile thinning via lower crustal flow and fold-induced doming in the West Carpathian Eo-Alpine collisional wedge. *Tectonics* 31, TC5002. https://doi.org/10.1029/2012TC003097

Kázmer M., Dunkl I., Frisch W., Kuhlemenn J. & Ozsvárt P. 2003: The Palaeogene forearc basin of the Eastern Alps and Western Carpathians: subduction erosion and basin evolution. *Journal of Geological Society* 160, 413–428. https://doi.org/10.1144/0016-764902-041

Kettner R. 1931: Géologie du versant nord de la Basse Tatra dans sa partie moyenne. *Knihovna Státniho Geologického Ústavu ČSR*, 13 A, 373–397.

Klinec A. 1976: Geological map of Slovenské rudohorie and the Nízke Tatry Mts. (1:50 000). *GÚDŠ*, Bratislava.

Kohút M., Stein H., Uher P., Zimmerman A. & Hraško Ľ. 2013: Re-Os and U–Th-Pb dating of the Rochovce granite and its mineralization (Western Carpathians, Slovakia). *Geologica Carpathica* 64, 71–79. https://doi.org/10.2478/geoca-2013-0005

Konečný V., Konečný P., Kubeš P. & Pécskay Z. 2015a: Paleovolcanic reconstruction of the Neogene Vepor stratovolcano (Central Slovakia), part I. *Mineralia Slovaca* 47, 1–76.

Konečný V., Konečný P., Kubeš P. & Pécskay Z. 2015b: Paleovolcanic reconstruction of the Neogene Vepor stratovolcano (Central Slovakia), part II. *Mineralia Slovaca* 47, 113–176.

Kováč M., Plašienka D., Soták J., Vojtko R., Oszczypko N., Less G., Ćosović V., Fügenschuh B. & Králiková S. 2016: Paleogene palaeogeography and basin evolution of the Western Carpathians, Northern Pannonian domain and adjoining areas. *Global and Planetary Change* 140, 9–27. https://doi.org/10.1016/j.gloplacha.2016.03.007

Kováč M., Márton E., Oszczypko N., Vojtko R., Hók J., Králiková S., Plašienka D., Klučiar T., Hudáčková N. & Oszczypko-Clowes M. 2017: Neogene palaeogeography and basin evolution of the Western Carpathians, Northern Pannonian domain and adjoining areas. *Global and Planetary Change* 155, 133–154. https://doi.org/10.1016/j.gloplacha.2017.07.004

Kováčik M., Kráľ J. & Maluski H. 1996: Metamorphic rocks in the Southern Veporicum basement: their Alpine metamorphism and thermochronologic evolution. *Mineralia Slovaca* 28, 185–202.

Kováčik M., Kráľ J. & Maluski H. 1997: Alpine reactivation of the southern Veporicum basement: metamorphism, $^{40}Ar/^{39}Ar$ dating, geodynamic model and correlation aspects with the Eastern Alps. In: Grecula P., Hovorka D. & Putiš M. (Eds.), Geological Evolution of the Western Carpathians. *Mineralia Slovaca – Monograph*, 163–174.

Kovács S., Sudan M., Grădinaru E., Gawlick H.-J., Karamata S., Haas J., Péró Cs., Gaetani M., Mello M., Polák M., Aljinović D., Ogorelec B., Kolar-Jurkovšek T., Jurkovšek J. & Buser S. 2011: Triassic Evolution of the Tectonostratigraphic Units of the Circum-Pannonian Region. *Jahrbuch der Geologischen Bundesanstalt* 151, 199–280.

Kozur H. & Mock R. 1973: Zum Alter and zur tektonischen stelung der Meliata-Serie des Slovakischen Karstes. *Geologický Zborník Geologica Carpathica* 24, 365–374.

Králiková S., Vojtko R., Hók J., Fügenschuh B. & Kováč M. 2016: Low-temperature constraints on the Alpine thermal evolution of the Western Carpathian basement rock complexes. *Journal of Structural Geology* 91, 144–160. https://doi.org/10.1016/j.jsg.2016.09.006

Kronome B. & Boorová D. 2014: Geological structure of the Tesná skala massif (Muránska planina, Central Western Carpathians) – results of geological mapping and biostratigraphic evaluation. *Geologické Práce*, *Správy* 123, 7–29 (in Slovak).

Lexa O., Schulmann K. & Ježek J. 2003: Cretaceous collision and indentation in the West Carpathians: View based on structural analysis and numerical modeling. *Tectonics* 22, 1066–1081. https://doi.org/10.1029/2002TC001472

Ložek V. 1960: Muráň breccia. *Věstník ÚÚG* 25, 469–471 (in Czech).

Lupták B., Thöni M., Janák M. & Petrík I. 2004: Sm–Nd isotopic chronometry of garnets from the Veporic Unit, Western Carpa-

thians: some preliminary age results and P-T constraints. *Geolines* 17, 66.

Madarás J., Putiš M. & Dubík B. 1994: Structural characteristics of the middle part of the Pohorelá tectonic zone; Veporicum, Western Carpathians. *Mineralia Slovaca* 26, 177–191 (in Slovak with English summary).

Madarás J., Hók J., Siman P., Bezák V., Ledru P. & Lexa O. 1996: Extension tectonics and exhumation of crystalline basement of the Veporicum unit (Central Western Carpathians). *Slovak Geological Magazine* 2, 179–183.

Maheľ M. 1957: Geology of the Stratenská hornatina Mts. [Geológia Stratenskej hornatiny]. *Geologické Práce*, *Zošit* 48, 1–200 (in Slovak).

Maheľ M., Kamenický J., Fusán O. & Matějka A. 1967: Regional geology of the ČSSR, II. part, Western Carpathians. *ČSAV*, Praha, 1–497.

Maheľ M. 1986: Geological structure of Czechoslovak Carpathians 1 – Paleoalpine units. *VEDA*, Bratislava, 1–503 (in Slovak).

Maluski H., Rajlich P. & Matte P. 1993: ^{40}Ar–^{39}Ar dating of the Inner Carpathians Variscan basement and Alpine mylonitic overprinting. *Tectonophysics* 223, 313–337. https://doi.org/10.1016/0040-1951(93)90143-8

Marko F. 1993: Kinematics of Muráň fault between Hrabušice and Tuhár village. *In:* Rakús M. & Vozár J. (Eds.): Geodynamický model a hlbinná stavba Západných Karpát. Konferencie, sympóziá, semináre. *Geol. Úst. D. Štúra*, Bratislava, 253–261.

Marko F. & Vojtko R. 2006: Structural record and tectonic history of the Mýto – Tisovec fault (Central Western Carpathians). *Geologica Carpathica* 57, 211–221.

Marko F., Plašienka D. & Fodor L. 1995: Meso-Cenozoic tectonic stress fields within the Alpine-Carpathian transition zone: a review. *Geologica Carpathica* 46, 19–27.

McClay K. 1987: The mapping of geological structures. *Open University Press*, London (reprint 1994), 1–161.

Mello J. 1979: Belong the higher Subtatric nappes and the Silica nappe to the Gemeric unit? *Mineralia Slovaca* 11, 279–281 (in Slovak).

Mello J., Filo I., Havrila M., Ivanička J., Madarás J., Németh Z., Polák M., Pristaš J., Vozár J., Koša E. & Jacko S. jun. 2000a: Geological map of the Slovenský raj, Galmus Mts. and Hornád Depression (M 1:50 000). *Geologický ústav Dionýza Štúra*, Bratislava.

Mello J., Filo I., Havrila M., Ivan P., Ivanička J., Madarás J., Németh Z., Polák M., Pristaš J., Vozár J., Vozárová A., Liščák P., Kubeš P., Scherer S., Siráňová Z., Szalaiová V. & Žáková E. 2000b: Explanations to Geological map of the Slovenský raj, Galmus Mts. and Hornád Depression (M 1:50 000). *Geologický ústav Dionýza Štúra*, Bratislava, 1–303 (in Slovak with English summary).

Mello J., Ivanička J., Grecula P., Janočko J., Jacko S. sen., Elečko M., Pristaš J., Vass D., Polák M., Vozár J., Vozárová A., Hraško Ľ., Kováčik M., Bezák V., Biely A., Németh Z., Kobulský J., Gazdačko Ľ., Madarás J. & Olšavský M. 2008: General geological map of the Slovak Republic (1:200 000), Map sheet 37 – Košice. *Ministry of Environment of the Slovak Republic*, *State Geological Institute of Dionýz Štúr*, Bratislava.

Michael A.J. 1984: Determination of stress from slip data: faults and folds. *Journal of Geophysical Research* 89, B13, 11517–11526. https://doi.org/10.1029/JB089iB13p11517

Milovský R., Hurai V., Plašienka D. & Biroň A. 2003: Hydrotectonic regime at soles of overthrust sheet: textural and fluid inclusion evidence from basal cataclasites of the Muráň nappe (Western Carpathians, Slovakia). *Geodinamica Acta* 16, 1–20. https://doi.org/10.1016/S0985-3111(02)00002-5

Mišík M. & Sýkora M. 1980: Jura der Silica-Einheit rekonstruktiert aus gerollen und oberkretazische Susswaser-Kalke des Gemerikum. *Geologický Zborník Geologica Carpathica* 31, 239–262.

Ondrejka M., LI X.-H., Vojtko R., Putiš M., Uher P. & Sobocký T. 2018: Permian A-type rhyolites of the Muráň Nappe, Inner Western Carpathians, Slovakia: in-situ zircon U–Pb SIMS ages and tectonic setting. *Geologica. Carpathica* 69, 187–198. https://doi.org/10.1515/geoca-2018-0011

Park R.G. 1993: Foundation of structural geology (2nd ed.). *Chapman & Hall*, New York, 1–148.

Pelech O. & Kronome B. 2019: Structural analysis in the wider zone of Muráň fault between Šumiac and Tisovec. *Geologické Práce*, *Správy* 134, 33–48 (in Slovak with English summary).

Pešková I., Vojtko R., Starek D. & Sliva Ľ. 2009: Late Eocene to Quaternary deformation and stress field evolution of the Orava region (Western Carpathians). *Acta Geologica Polonica* 59, 73–91.

Petit J.P. 1987: Criteria for the sense of movement on fault surfaces in brittle rocks. *Journal of Structural Geology* 9, 597–608. https://doi.org/10.1016/0191-8141(87)90145-3

Plašienka D. 1993: Structural pattern and partitioning of deformation in the Veporic Foederata cover unit (Central Western Carpathians). In: Rakús M. & Vozár J. (Eds.): Geodynamic model and deep structure of the Western Carpathians. *Konf. Symp. Sem., GÚDŠ*, Bratislava, 269–277.

Plašienka D. 1999: Tectonochronology and paleotectonic model of the Jurassic to Cretaceous evolution of the Central Western Carpathians. *VEDA*, Bratislava, 1–127 (in Slovak with English summary).

Plašienka D. 2003: Development of basement-involved fold and thrust structures exemplified by the Tatric–Fatric–Veporic nappe system of the Western Carpathians (Slovakia). *Geodinamica Acta* 16, 21–38. https://doi.org/10.1016/S0985-3111(02)00003-7

Plašienka D. 2018: Continuity and episodicity in the early Alpine tectonic evolution of the Western Carpathians: How large-scale processes are expressed by the orogenic architecture and rock record data. *Tectonics* 37, 2029–2079. https://doi.org/10.1029/2017TC004779

Plašienka D. & Soták J. 1996: Rauhwackized carbonate tectonic breccias in the West Carpathian nappe edifice: introductory remarks and preliminary results. *Slovak Geological Magazine* 3–4, 287–291.

Plašienka D. a Soták J. 2001: Stratigraphic and tectonic position of Carboniferous sediments in the Furmanec Valley (Muráň Plateau, Central Western Carpathians). *Mineralia Slovaca* 33, 29–44 (in Slovak).

Plašienka D., Grecula P., Putiš M., Kováč M. & Hovorka D. 1997: Evolution and structure of the Western Carpathians: an overview. In: Grecula P., Hovorka D. & Putiš M. (Eds.): Geological evolution of the Western Carpathians. *Mineralia Slovaca – Monograph*, Bratislava, 1–24.

Plašienka D., Broska I., Kissová D. & Dunkl I. 2007: Zircon fission-track dating of granites from the Vepor-Gemer Belt (Western Capathians): constraints for the Early Alpine exhumation history. *Journal of Geoscience* 52, 113–123. https://doi.org/10.3190/jgeosci.009

Poller U., Uher P., Janák M., Plašienka D. & Kohút M. 2001: Late Cretaceous age of the Rochovce granite, Western Carpathians, constrained by U–Pb single-zircon dating in combination with cathodoluminiscence imaging. *Geologica Carpathica* 52, 41–47.

Poller U., Uher P., Broska I., Plašienka D. & Janák M. 2002: First Permian–Early Triassic zircon ages for tin-bearing granites from the Gemeric unit (Western Carpathians, Slovakia): connection to the post-collisional extension of the Variscan orogen and S-type granite magmatism. *Terra Nova* 14, 41–48. https://doi.org/10.1046/j.1365-3121.2002.00385.x

Pospíšil L., Nemčok J., Graniczny M. & Doktór S. 1986: Contribution of remote sensing to the identification of the strike-slip

faults in the West Carpathians. *Mineralia Slovaca* 18, 358–402 (in Czech).

Pospíšil L., Bezák V., Nemčok J., Feranec J., Vass D. & Obernauer D. 1989: The Muráň tectonic system as example of horizontal displacement in the West Carpathians. *Mineralia Slovaca* 21, 305–322 (in Slovak).

Pulec M. 1966: Geological research of the Tertiary in the intramontane basins of the Central Western Carpathians. *Manuscript – archive Geofond*, Bratislava (in Slovak).

Putiška R., Dostál I., Mojzeš A., Gajdoš V., Rozimant K. & Vojtko R. 2012: The resistivity image of the Muráň fault zone (Central Western Carpathians) obtained by electrical resistivity tomography. *Geologica Carpathica* 63, 233–239. https://doi.org/10.2478/v10096-012-0017-3

Radvanec M., Konečný P., Ondrejka M., Putiš M., Uher P. & Németh Z. 2009: The Gemeric granites as an indicator of the crustal extension above the Late-Variscan subduction zone and during the Early Alpine riftogenesis (Western Carpathians): an interpretation from the monazite and zircon ages dated by CHIME and SHRIMP methods. *Mineralia Slovaca* 41, 381–394 (in Slovak with English summary).

Radvanec M., Németh Z., Kráľ J. & Pramuka S. 2017: Variscan dismembered metaophiolite suite fragments of Paleo-Tethys in Gemeric unit, Western Carpathians. *Mineralia Slovaca* 49, 1–48.

Rakús M. 1996: Jurassic of the innermost Western Carpathian zone – its importance and influence on the geodynamic evolution of the area. *Slovak Geological Magazine* 3–4, 311–317.

Rakús M. & Sýkora M. 2001: Jurassic of Silicicum. *Slovak Geological Magazine* 7, 53–84.

Ramsay J. G. & Graham R. H. 1970: Strain variation in shear belts. *Canadian Journal of Earth Sciences* 7, 786–813. https://doi.org/10.1139/e70-078

Reichwalder P. 1982: Structural characteristic of the root zone of some nappes in innermost parts of West Carpathians. In: Maheľ M. (Ed.): Alpine structural elements: Carpathian–Balkan–Caucasus–Pamir orogene zone. *VEDA*, Bratislava, 43–56.

Riedel W. 1929: Zur Mechanik geologischer Brucherscheinungen ein Beitrag zum Problem der Fiederspatten. *Zentralblatt für Mineralogie, Geologie und Paläontologie Abt.* 354–368.

Royden L.H. & Báldi T. 1988: Early Cenozoic tectonics and paleogeography of the Pannonian Basin and surrounding regions. *American Association of Petroleum Geologists Memoirs* 45, 1–16. https://doi.org/10.1306/M45474C1

Schönnenberg R. 1946: Geologische Untersuchungen an nord-westerland des Zips-Gomorer Erzgebirges (Karpaten). *Zeitschrift der Deutschen Geologischen Gesellschaft* 98, 70–120. https://doi.org/10.1127/zdgg/98/1948/70

Soták J., Bebej J. & Biroň A. 1996: Detrital analyse of the Paleogene flysch deposits of the Levoča Mts: evidence for sources and paleogeography. *Slovak Geological Magazine* 2, 345–349.

Soták J., Pereszlényi M., Marschalko R., Milička J. & Starek D. 2001: Sedimentology and hydrocarbon habitat of the submarine-fan deposits of the Central Carpathian Paleogene Basin (NE Slovakia). *Marine and Petroleum Geology* 18, 87–114. https://doi.org/10.1016/S0264-8172(00)00047-7

Soták J., Plašienka D. & Vojtko R. 2005: Paleogene sediments of the Vepor belt – biostratigraphic data from new occurrences at the NNW of Tisovec. *Mineralia Slovaca – Geovestník* 37, 13–14 (in Slovak).

Sůkalová Ľ., Vojtko R. & Pešková I. 2012: Cenozoic deformation and stress field evolution of the Kozie chrbty Mountains and the western part of Hornád Depression (Central Western Carpathians). *Acta Geologica Slovaca* 4, 53–64.

Uhlig V. 1903: Bau und bild der Karpaten. In: Diener K., Hoernes R., Suess F.E. & Uhlig V. (Eds.): Bau un Bild der Österreich. *Verl. F. Tempsky*, Wien, 651–991.

Vavryčuk V. 2014: Iterative joint inversion for stress and fault orientations from focal mechanisms. *Geophysical Journal International* 199, 69–77. https://doi.org/10.1093/gji/ggu224

Vojtko R. 2000: Are there tectonic units derived from the Meliata–Hallstatt trough incorporated into the tectonic structure of the Tisovec Karst? (Muráň karstic plateau, Slovakia). *Slovak Geological Magazine* 6, 335–346.

Vojtko R. 2003: Fault-slip analysis and geodynamical evolution of the central part of Slovenské rudohorie Mts. *PhD. Thesis*, *Comenius Univ. Dept. Geol. & Paleont.*, Bratislava, 1–124 (in Slovak).

Vojtko R., Tokárová E., Sliva Ľ. & Pešková I. 2010: Cenozoic palaeostress field reconstruction and revised tectonic history in the northern part of the Central Western Carpathians (the Spišská Magura and Tatra Mountains). *Geologica Carpathica* 61, 211–225. https://doi.org/10.2478/v10096-010-0012-5

Vojtko R., Králiková S., Kriváňová K. & Vojtková S. 2015: Lithostratigraphy and tectonics of the eastern part of the Veporské vrchy Mts. (Central Western Carpathians). *Acta Geologica Slovaca* 7, 113–127.

Vojtko R., Králiková S., Jeřábek P., Schuster R., Danišík M., Fügenschuh B., Minár J. & Madarás J. 2016: Geochronological evidence for the Alpine tectono-thermal evolution of the Veporic Unit (Western Carpathians, Slovakia). *Tectonophysics* 666, 48–65. https://doi.org/10.1016/j.tecto.2015.10.014

Vozárová A. 1993: Variscan metamorphism and crustal evolution in the Gemericum. *Západné Karpaty*, *Séria Mineralógia Petrológia Geochémia Metalogenéza* 16, 55–117 (in Slovak).

Vozárová A. 1995: Spätné násuny na severnom okraji gemerika [Reverse thrusts at northern margin of the Gemericum Unit]. *Geologické Práce*, *Správy* 100, 119–123.

Vozárová A. & Vozár J. 1988: Late Palaeozoic in West Carpathians. *Monogr., D. Štúr Geol. Inst.*, Bratislava, 1–314.

Vozárová A. & Rojkovič I. 2000: Permian lacustrine phosphatic sandstone in the Southern Gemeric unit, Western Carpathians, Slovakia. *Geologica Carpathica* 51, 265–278.

Vrána S. 1980: Newly-formed Alpine garnets in metagranitoids of the Veporides in relation to the structure of the Central zone of the West Carpathians. *Časopis pro Mineralogii a Geologii* 25, 41–54.

Wallace R.E. 1951: Geometry of shearing stress and relation to faulting. *Journal of Structural Geology* 59, 118–130. https://doi.org/10.1086/625831

Zoubek V. 1957: Hranice gemerid s veporidami [Boundaries between the Gemerides and Veporides]. *Geologické Práce*, *Zošit* 46, 38–43.